

Home Search Collections Journals About Contact us My IOPscience

High-power semiconductor separate-confinement double heterostructure lasers

This article has been downloaded from IOPscience. Please scroll down to see the full text article.

2010 Quantum Electron. 40 661

(http://iopscience.iop.org/1063-7818/40/8/R02)

View the table of contents for this issue, or go to the journal homepage for more

Download details:

IP Address: 159.226.100.225

The article was downloaded on 12/04/2011 at 09:16

Please note that terms and conditions apply.

REVIEW

PACS numbers: 42.55.Px; 42.60.Jf; 42.60.Lh DOI: 10.1070/QE2010v040n08ABEH014375

High-power semiconductor separate-confinement double heterostructure lasers

I.S. Tarasov

Contents	
1. Introduction	661
2. Semiconductor lasers with small internal optical losses	663
2.1 Internal optical losses in SC DHs	
2.2 Higher order mode selection in asymmetric SC DHs	
2.3 Internal optical losses in an asymmetric SC DH	
2.4 High-power semiconductor lasers based on an asymmetric SC DH	
3. Temperature delocalisation of charge carriers in SC DHs	667
3.1 Overheating of the active region in a cw semiconductor laser	
3.2 Temperature dependence of internal optical losses	
4. Basic foundations of the concept of high-power semiconductor lasers	670
5. Internal quantum yield and effect of the active region thickness on this yield	670
6. Catastrophic optical degradation and optical power density	671
7. Quenching of lasing in semiconductor lasers with small internal optical losses	672
8. Pulsed semiconductor lasers	673
8.1 Pulsed lasing and fundamental limit of the optical power confinement of a semiconductor laser	
8.2 Fundamental limit of the optical power confinement of a semiconductor laser	
8.3 Injection of charge carriers into the waveguide layer at high pump powers	
8.4 Epitaxial tunnel-coupled laser structures	
9. High-power semiconductor lasers with a distributed Bragg mirror	677
10. Conclusions. Fundamental, design, and technological factors	
affecting the limiting parameters of high-power semiconductor lasers	678
11. References	678

Abstract. The review is devoted to high-power semiconductor lasers. Historical reference is presented, physical and technological foundations are considered, and the concept of high-power semiconductor lasers is formulated. Fundamental and technological reasons limiting the optical power of a semiconductor laser are determined. The results of investigations of cw and pulsed high-power semiconductor lasers are presented. Main attention is paid to inspection of the results of experimental studies of single high-power semiconductor lasers. The review is mainly based on the data obtained in the laboratory of semiconductor luminescence and injection emitters at the A.F. Ioffe Physical-Technical Institute.

I.S. Tarasov A.F. Ioffe Physical-Technical Institute, Russian Academy of Sciences, ul. Politekhnicheskaya 26, 194021 St. Petersburg, Russia; e-mail: tarasov@hpld.ioffe.ru

Received 4 June 2010 *Kvantovaya Elektronika* **40** (8) 661–681 (2010) Translated by I.A. Ulitkin Keywords: semiconductor laser, separate-confinement heterostructure, asymmetric double heterostructure, internal optical losses, temperature delocalisation, internal quantum yield, fundamental limit on the optical power of a semiconductor laser, epitaxial tunnel-coupled laser structure, distributed Bragg mirror.

1. Introduction

For more than fifty years semiconductor physics and technology have been the site of bright events [1-11] associated with the development of semiconductor lasers. Among these events there are landmarks which resulted in the appearance of new types of semiconductor lasers with strongly pronounced characteristic features [12-16]. However, they all emerged most often after drastic improvement of one of the parameters and deterioration of some others. These are single-mode lasers [17, 18], single-frequency semiconductor lasers [12, 13], lasers emitting ultrashort pulses [19, 20], superluminescent diodes with a broad emission spectrum [21, 22], etc. The line of high-power semiconductor lasers could not be formed for a long time because the required increase in the power contradicted one

of the main advantages of semiconductor lasers, namely compactness. But after it was shown that miniature lasers can be powerful [23–25], the line of high-power semiconductor lasers has finally come into being. The main distinctive feature of high-power semiconductor lasers is the possibility of improving the power characteristics without deterioration of some other parameters.

High-power semiconductor lasers are based on separateconfinement double heterostructures (SC DHs) (Fig. 1). Initially the SC DH was aimed at confining an electromagnetic wave by a waveguide layer and at decreasing the threshold current density due to a decrease in the active region thickness. The use of a quantum-well epitaxial layer as an active region of the laser SC DH allowed one to reduce the threshold current density first down to 160 A cm⁻² [26] and then down to 40 A cm⁻² [27]. In this case, the optical confinement factor was increased by fabricating a 0.15-0.25-µm-thick waveguide. In order to minimise the threshold current, the number of quantum-well layers in the active region was increased up to four or six, which also made it possible to increase the optical confinement factor and the mode gain at minimal lengths of the Fabry-Perot resonator.

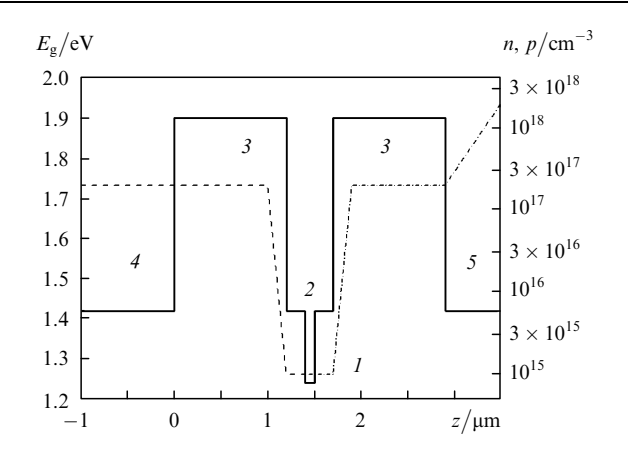


Figure 1. Schematic energy band diagram of the InGaP/GaAs/InGaAs SC DH (the laser wavelength, $\lambda \sim 1~\mu m$) (solid line) and the calculated doping profiles for the silicon donor impurity (dashed line) and magnesium acceptor impurity (dash-and-dot line), z is the coordinate of the structure growth [(1) the active region (an InGaAs quantum well); (2) the GaAs waveguide; (3) InGaP emitters; (4) GaAs substrate; (5) contact layer].

To obtain quantum-well layers, several variants of the liquid phase epitaxy methods were proposed [9, 28, 29] allowing one to produce layers in a system of InGaAsP/ GaAs and InGaAsP/InP quadruple solid solutions. The modified liquid phase epitaxy method from a moving solution-melt [29] became the most widespread. Application of this method for fabricating laser SC DHs with extended waveguides made it possible to find the anomalous dependence of the threshold current density on the Fabry-Perot resonator length in the case of optical excitation, which eliminated the influence of the doping processes on the laser structure homogeneity [30]. The use of dopants with a small diffusion coefficient for producing laser structures attested to the presence of the anomalous dependence of the threshold current density on the resonator length but already in the case of injection pumping [31]. Anomalously small threshold current densities at larger resonator lengths ($L=1000-2000~\mu m$) and anomalously high threshold current densities at standard lengths of the resonator ($L=250-350~\mu m$) indicated that it is possible to compensate for the drawback in radiation amplification due to an increase in the resonator length of a separate-confinement heterostructure semiconductor laser with an extended waveguide.

The possibility of decreasing internal optical losses did not seem obvious for a long time because of a large difference (more than two orders of magnitude) between the internal optical losses in the laser heterostructure and the gain of the semiconductor material of the active region. Therefore, the idea of increasing the pump current by perfecting technologically the epitaxial layers and heterojunctions of the laser structure was basic in designing highpower semiconductor lasers. All the attempts aimed at improving technologically the laser heterostructures in an effort to increase the resonator length had a relative success. An increase in the Fabry-Perot resonator length of a 'classical' (with a thin waveguide) semiconductor laser demonstrated a decrease in the slope quantum efficiency and a decrease in the output power. This can be easily explained by analysing the well-known expression for the external slope quantum efficiency η_d of a semiconductor Fabry-Perot laser

$$\eta_{\rm d} = \eta_{\rm int} \frac{\alpha_{\rm ext}}{\alpha_{\rm int} + \alpha_{\rm ext}}.$$
 (1)

It follows from this expression that a decrease in the internal optical losses $\alpha_{\rm int}$ can retain the high slope quantum efficiency of a semiconductor laser with a long resonator. Here, $\eta_{\rm int}$ is the internal quantum yield of stimulated emission; $\alpha_{\rm ext} = (2L)^{-1} \ln{(1/R_1R_2)}$ are the useful optical losses at the output; L is the resonator length; R_1 and R_2 are the reflectivities of the Fabry–Perot resonator mirrors.

The further development of the modified liquid phase epitaxy method made it possible to produce laser SC DHs with quantum-well active regions and to reduce the threshold current densities down to $300-400~{\rm A}~{\rm cm}^{-2}$ in long lasers [30, 32, 33]. Nevertheless, of key importance were experimental works proving the possibility of retaining the high slope quantum efficiency in lasers with long (at that time) resonators ($1500-2500~{\mu m}$) and an extended waveguide [34, 35].

Therefore, the waveguide expansion in the laser SC DH allows one to decrease internal optical losses and to increase the resonator length of a semiconductor laser, which ensures the maximum current passage through a laser diode and thus the achievement of the maximal output power. This principle, the basic one in the concept of creation of highpower SC DH semiconductor lasers with an extended waveguide, was first experimentally realised in [36]. The authors of this paper, using the modified liquid phase epitaxy method, fabricated a semiconductor laser with a 100-µm aperture and a 1.16-mm-long resonator, whose output power in the cw regime was 5 W at a maximal efficiency of 50 %.

The further development of semiconductor lasers was due to perfection of new epitaxial technologies: MOS hydride epitaxy and molecular beam epitaxy.

2. Semiconductor lasers with small internal optical losses

2.1 Internal optical losses in SC DHs

In a laser diode as in any other laser, the lasing regime sets in when all the losses are compensated for by amplification. In modern laser heterostructures the current leakage is reduced to minimal, while the internal quantum yield in the active region achieves virtually 100%. To this end, the main attention is paid to optical losses – internal optical losses $\alpha_{\rm int}$ and useful optical losses at the resonator output $\alpha_{\rm ext}$. The value of $\alpha_{\rm ext}$ is completely determined by the mirror reflectivities and the resonator length of the semiconductor laser. The authors of papers [37, 38] were the first to consider internal optical losses and possible ways of their reduction.

Internal optical losses are convenient to consider as a sum of losses in each layer of the laser heterostructure (Fig. 1) and scattering losses α_s from the inhomogeneities of epitaxial layers:

$$\alpha_{\rm int} = \sum \sum \Gamma_{jm} \alpha_j + \alpha_{\rm s},$$
(2)

where Γ_{jm} is the optical confinement factor for the *m*th mode in the *j*th layer; α_j are the scattering losses on free charge carriers in the *j*th layer. Note that the scattering losses from the inhomogeneities of the epitaxial layers in modern laser structures are assumed negligibly small.

Outside the lasing threshold radiation scattering by free charge carriers leads to intraband transitions and increases with increasing concentration of the charge carriers and wavelength of absorbed light. The type of particles participating in the pulse scattering determines the exponent k in the dependence of the scattering coefficient by free charge carriers on the laser radiation wavelength: $\alpha_i \sim \lambda^k$ [39]. In weakly doped semiconductor epitaxial layers, which are waveguide layers, the pulse is mainly scattered by optical phonons and linearly depends on the concentration of charge carriers [40], and in heavily doped layers (these are emitter layers of the leaser heterostructure), the dependence is quadratic [40]. The minimal doping level of a waveguide layer of the laser structure and the active region is determined by the epitaxial technology being employed. Outside the lasing threshold the charge carrier concentration corresponds to the threshold one. The emitter layers are doped up the level providing an efficient injection of positive and negative charge carriers and a minimal series resistance.

The total internal losses can be reduced by decreasing the optical confinement factor for the emitter layers and the active region layer. The simplest method to do this is the expansion of the waveguide layer, which was demonstrated in investigations of the separate-confinement laser heterostructures on GaAs [37] and InP [38] substrates. Figure 2 presents the dependence of the optical confinement factors for emitter layers and the active region layer on the waveguide layer thickness [38]. The waveguide expansion leads to a decrease in both optical confinement factors but the emergence of higher-order modes serves as its limit. Due to this, the waveguide thickness in a symmetric laser SC DH is limited by 0.7–1.0 µm. But even this increase in the waveguide thickness allows one to decrease significantly the internal optical losses. Figure 3 shows the calculated

dependences of the internal optical losses in SC DH lasers on the resonator length and the waveguide thickness [38]. The internal optical losses were calculated using the expression [41]:

$$\alpha_{\rm int} = \sigma_n n + \sigma_{\rm p} p,\tag{3}$$

where n, p are the volume concentrations of electrons and holes; σ_n , σ_n are the cross sections of scattering by free electrons and holes whose values for gallium arsenide were taken from experimental paper [41], for indium phosphate – from paper [42], and for the active region GaInAs – from paper [43]. To decrease the internal optical losses in laser heterostructures (especially on InP substrates) it is needed to decrease the concentration of nonequilibrium charge carriers in waveguide layers as well as the fraction of electromagnetic radiation in heavily doped layers (especially in the p emitter). This can be done by two ways. The first method is based on the waveguide expansion, which leads to some increase in the threshold current density but provides an efficient decrease in the total internal optical losses. The second method is associated with an increase in the refractive index step at the waveguide-emitter interface, which results in a decrease of electromagnetic field penetration in the emitter layers. However, the set of semiconductor solid solutions used for fabricating laser heterostructures is often limited by the list of initial semiconductor compounds or by the isoperiodicity require-

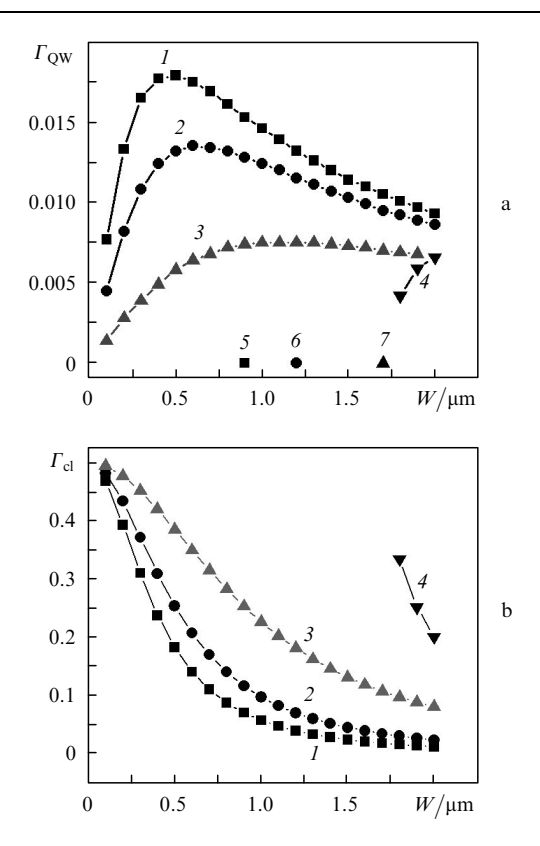


Figure 2. Dependence of the optical confinement factor of the active-region layer $\Gamma_{\rm QW}$ (a) and emitter layer $\Gamma_{\rm cl}$ (b) for zero (1,2,3) and second (4) modes on the InGaAsP-waveguide thickness W for three InGaAsp/InP SC DHs at the energy-gap width of the waveguide solid solution 1.1 eV (1,4,5), 1.2 eV (2,6), and 1.3 eV (3,7). Points on the abscissa show the waveuide thicknesses at which the first odd mode appears.

ment. Thus, the maximal step in the refractive index at the waveguide–emitter interface (Δn) is limited by the requirement of a sufficient quantum-well depth of the active region, which noticeably narrows down the possibilities of the second method. In symmetric SC DHs the combination of both approaches allowed one to decrease the internal optical losses by three–five times down to 1.5 cm⁻¹. This decrease in the internal optical losses in laser structures was experimentally realised with the help of metal-organic vapour phase epitaxy [24, 44–47]. In these papers, due to a decrease in the internal optical losses, the ten-watt level of the cw power generated by a multimode laser with a mesastripe width $D=100~\mu m$ was surmounted.

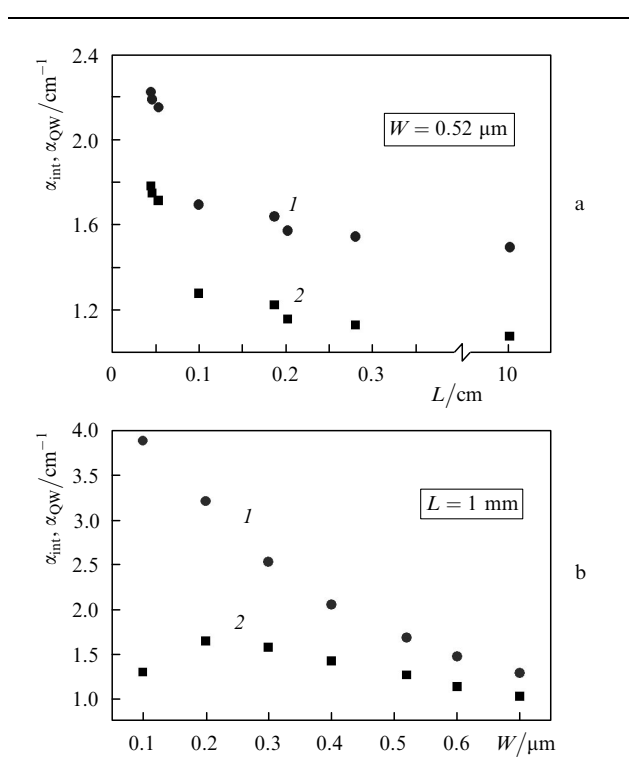


Figure 3. Dependences of the total internal optical losses $\alpha_{\rm int}$ (1) and optical losses in the active region $\alpha_{\rm QW}$ (2) on the laser-diode resonator length L (a) and on the waveguide thickness W (b) in the structure presented in Fig. 1.

2.2 Higher-order mode selection in asymmetric SC DHs

Above we have considered in detail symmetric separateconfinement laser heterostructure with low internal losses. The natural limitation on the symmetric waveguide thickness of such a heterostructure is the fulfilment of threshold conditions for waveguide higher-order modes [37, 38, 48], which occurs due to a decrease in their losses at the output (Fig. 4). The reflectivity for different transverse modes depends on the waveguide thickness [49-54]. Using the dependence of the internal optical losses in the waveguide thickness (Fig. 3b), Slipchenko et al. [55] calculated the threshold concentration of charge carriers in the active region for the fundamental mode and higher-order modes versus the waveguide thickness for a symmetric laser SC DH (Fig. 5). It follows from Fig. 5 that in the case of thick $(W \ge 1.5 \,\mu\text{m})$ waveguide layers and long $(L = 4 \,\text{mm})$ Fabry-Perot resonators, the difference between the threshold concentrations of the fundamental mode and higherorder modes does not exceed 10 %. In calculating the threshold concentration, the influence of many parameters was taken into account, including the waveguide efficiency (step Δn) and laser radiation wavelength λ , which determine the quantity and character of the dependence of the reflectivity on the waveguide thickness and the laser resonator length. The experimentally found difference of threshold concentrations of the fundamental mode and the higher-order modes did not exceed 1.8 % -6.4 % [55] for thick waveguide layers and long (more than 4 mm) Fabry – Perot resonators. In laser diodes this small discrepancy in the threshold concentrations leads to the possibility of simultaneous fulfilment of threshold conditions for the modes. This occurs due to fluctuations of the charge carrier concentrations in the quantum well and due to some increase in the threshold concentration outside the lasing threshold. In this case, several transverse modes are excited in symmetric superwide waveguides.

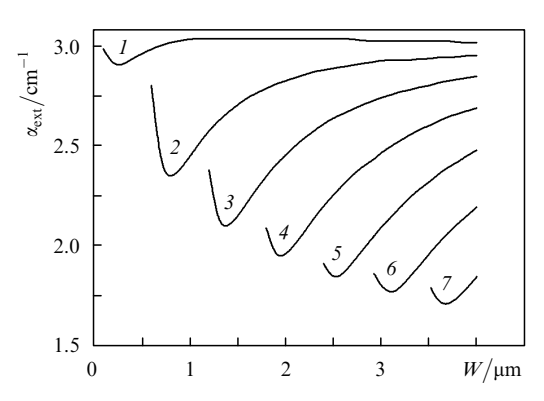


Figure 4. Dependences of the external optical losses $\alpha_{\rm ext}$ on the waveguide thickness W for the zero (1), first (2), second (3), third (4), fourth (5), sixth (6), and seventh (7) modes of laser diodes with a 4-mm-long resonator. The radiation wavelength is $\lambda=1.06~\mu{\rm m}$.

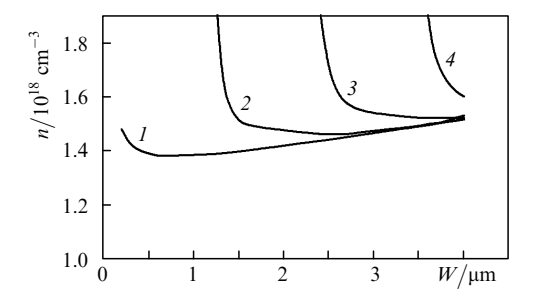


Figure 5. Dependences of the threshold electron concentrations n on the waveguide thickness W for the zero (1), second (2), fourth (3), and sixth (4) modes of laser symmetric heterostructures. The laser-diode resonator length is 4 mm and the radiation wavelength is $\lambda = 1.06 \ \mu m$.

Several methods of higher-order mode selection are known. The first method is associated with an increase in losses in heavily doped emitter layers [37]. In the second method, the higher-order modes are selected by using the design ensuring the mode leakage from the main waveguide [56]. In the third method, the higher-order mode selection is performed due to the difference in the radiation losses at the resonator output through an AR-coated mirror, which is achieved by deviating radiation from the waveguide axis for the higher-order modes [49].

To realise these methods, some works were performed to fabricate laser extended-waveguide SC DHs retaining generation of only the fundamental transverse mode [37, 57-61]. The best results related to the mode suppression and the decrease in the radiation divergence were achieved by using the mode leakage from the laser heterostructure waveguide [37, 61]. However, as in other cases known to us, the employed solutions lead to an increase in technological requirements, an increase in the internal losses and a decrease in the optical power [37, 57–61]. The higher-order modes were most successfully suppressed in an asymmetric quantum-well SC DH [55]. The authors of paper [62] realised for the first time a laser with a single-mode superwide asymmetric waveguide in an effort to decrease simultaneously the internal optical losses and radiation divergence in the plane perpendicular to the p-n junction. An increase in the waveguide thickness up to 4 µm made it possible to decrease the internal optical losses down to 0.7 cm⁻¹ and the radiation divergence down to 16°-18° without a noticeable reduction in the maximal output power, which was 8.6 W.

The authors of paper [55] considered in detail the higherorder mode selection in an expanded waveguide based on the asymmetric SC DH due to a decrease in the optical confinement factors for these modes. The main idea of paper [55] becomes clear when considering the threshold conditions separately for each transverse mode of an expanded strip waveguide of the laser structure.

The lasing threshold condition in a laser can be written in the form [41]:

$$\Gamma_{\text{QW}}g(n_{\text{QW}}, p_{\text{QW}}) = \alpha_{\text{int}} + \alpha_{\text{ext}},$$
 (4)

where $g(n_{\rm QW}, p_{\rm QW})$ is the material gain in the active medium; $n_{\rm QW}$, $p_{\rm QW}$ are the threshold concentrations of electrons and holes; $\Gamma_{\rm QW}$ is the optical confinement factor in the active region. It follows from expression (4) that the fulfilment of the threshold conditions can be affected by varying the threshold concentrations of free charge carriers, the optical confinement factor for the corresponding mode or the balance of total optical losses between the fundamental mode and the higher-order modes.

As an example, the authors of paper [55] considered a standard laser SC DH with the emitters from the Al_{0.3}Ga_{0.7}As solid solution and the waveguide thickness of 1.7 µm. In this case, the waveguide equation has three solutions to which three stable field configurations correspond. In such a laser heterostructure the optical confinement factor of the active region for the mth mode $\Gamma_{\text{OW}m}$ weakly differs from that for the fundamental mode $\Gamma_{\rm OW0}$ and higher-order modes. At the same time, the optical confinement factor of the active region depends variously on its position in the waveguide layer for different modes (Fig. 6). There exist such positions of the active region in the waveguide for which the optical confinement factor in this region is higher for the fundamental mode than for the higher-order modes (Fig. 6). If the ratio $\Gamma_{\rm QW0}/\Gamma_{\rm QWm}$ provides a sufficient difference between threshold concentrations of the fundamental mode and the higher-order modes, the threshold conditions for the mth mode will not be fulfilled. The quantity of the active region shift with respect to the waveguide centre (this quantity characterises the optimal position) monotonically increases with the waveguide thickness (Fig. 7), but when it becomes resonant for the emergence of a new higher-order mode, the depend-

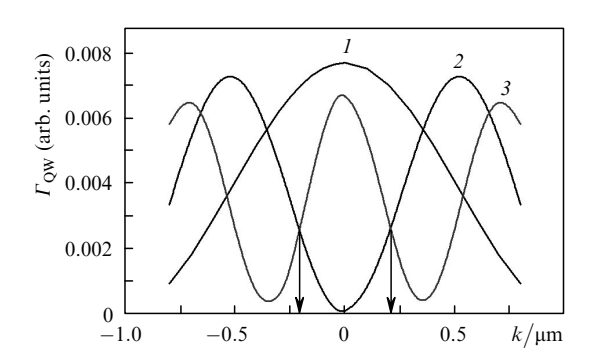


Figure 6. Dependences of the optical confinement factor $\Gamma_{\rm QW}$ for the active region on its position in the waveguide k for the zero (1), first (2), and second (3) modes. Calculations were performed for the laser heterostructure with $\lambda=1.06~\mu{\rm m}$ and the waveguide thickness $W=1.7~\mu{\rm m}$. Arrows show the positions of the active region with the maximal ratio $\Gamma_{\rm QW0}/\Gamma_{\rm QWm}$ (m is the mode number).

ence demonstrates a sharp dip. Figure 7 also presents the dependence of the ratio $\Gamma_{\rm QW0}/\Gamma_{\rm QWm}$ for the optimal position of the active region on the waveguide thickness. An increase in the waveguide layer thickness is accompanied by a decrease in its selective ability.

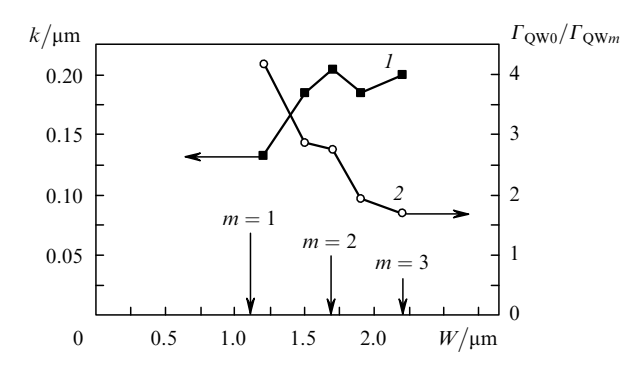


Figure 7. Dependences of the optimal displacement of the active region with respect to the waveguide centre (1) and well as of the ratios $\Gamma_{\text{QW0}}/\Gamma_{\text{QWm}}$ (2) on its thickness for laser heterostructures with $\lambda = 1.06 \ \mu\text{m}$. Arrows show the thicknesses at which the first (m=1), second (m=2), and third (m=3) modes appear.

Thus, the active region shift in a laser SC DH makes it possible to suppress the generation of the higher-order modes due to a decrease in their optical confinement factors and to expand the waveguide up to $4 \mu m$ and event larger.

2.3 Internal optical losses in an asymmetric SC DH

The internal optical losses in symmetric and asymmetric laser SC DHs are virtually identical and are calculated using expressions (2) and (3). The structure asymmetry makes it possible to remove limitations on the waveguide thickness and to expand it (i.e. to increase its thickness) up to 4 µm because the further expansion will lead to the problem of the transport of charge carriers in the waveguide layer and to an increase in the series resistance. The laser structure asymmetry weakly affects the optical confinement factor and the internal optical losses in the active region for the fundamental transverse mode and virtually has little effect on them in the waveguide and emitter layers. This occurs because the shift of the active

region in the waveguide influences mainly the optical confinement factor of the higher-order modes while other parameters of the structure remain the same.

The estimate of the maximal decrease in the internal optical losses in an asymmetric laser heterostructure is of special interest in designing high-power semiconductor lasers. Below we present a quantitative assessment of the total internal losses α_{int} for symmetric and asymmetric laser heterostructures as a function of the waveguide thickness [55]. To calculate α_{int} it is necessary to know the optical confinement factors of the mode for each structure layer, the absorption cross sections for electrons and holes as well as charge carrier concentrations. The dependences of the optical confinement factors were calculated taking into account geometrical and material factors of laser structures [55]. Use was also made of the scattering cross section for electrons and holes $\sigma_n = 3 \times 10^{-18} \text{ cm}^2$ and $\sigma_p = 7 \times 10^{-18} \text{ cm}^2$ 10⁻¹⁸ cm² [63] as well as of typical concentrations of the dopants in the laser heterostructure with the parameters specified by the technological process. N- and P-type conduction emitters had the concentration of the electrons $N = 10^{18} \text{ cm}^{-3} \text{ and holes } P = 3.5 \times 10^{18} \text{ cm}^{-3}.$ The waveguide layers were assumed undoped, the concentration of the residual dopant being 3×10^{15} cm⁻³.

In the waveguide layers of both heterostructures $\alpha_{\rm int}$ was of the order of $0.03 {\rm cm}^{-1}$ in the entire range of waveguide thickness $(1-4~\mu m)$. This is caused by the fact that the optical confinement factor for the waveguide layers is virtually independent of the waveguide layer thickness (except the regions where new higher-order modes appear). The internal optical losses in the waveguide can be decreased only by decreasing the doping level of epitaxial layers [55].

The waveguide expansion allows one to decrease the optical confinement factor and internal optical losses in the emitter layers if the penetration depth of the mode field in the emitters is reduced down to submicron values. The depth of the field penetration in the emitters is noticeably affected by the waveguide efficiency (the step Δn). Other doping conditions being the same, the losses in the emitters α_{cl} will be larger for the structures with a smaller step Δn at the waveguide-emitter interface. Unlike the active region, the concentration of free charge carriers in the emitters is specified during the technological growth of the laser heterostructure; therefore, its value can be varied in a wide range at the waveguide boundaries. Optimisation of the distribution profile of the free charge carrier concentration in the emitter layers can be an efficient tool for decreasing α_{cl} . Thus, using superwide waveguides and optimised profiles of emitter doping, we can minimise the contribution of α_{cl} to the total internal losses. The dependences of the fraction of internal optical losses in the emitter layers on the waveguide thickness are presented in Fig. 8 [55].

The internal optical losses $\alpha_{\rm QW}$ in the specified active region material, which is characterised by the scattering cross sections of the holes σ_p and electrons σ_n , depend on the optical confinement factor $\Gamma_{\rm QW}$ and the concentration of free carriers $n_{\rm QW}$ and $p_{\rm QW}$. An increase in the waveguide layer thickness leads to a decrease in the optical confinement factor in the active region (quantum well) for the fundamental mode. However, $\Gamma_{\rm QW}$, $n_{\rm QW}$, and $p_{\rm QW}$ in the quantum well are coupled by the threshold lasing condition (4). It follows that in the case of a semiconductor laser with fixed internal and external optical losses it is impossible to

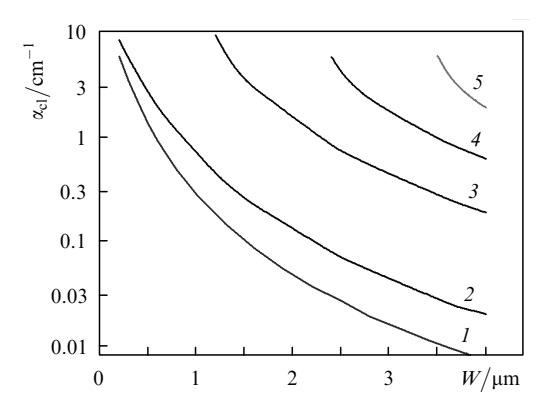


Figure 8. Dependences of the internal optical losses in two emitter layers α_{cl} on the waveguide thickness for the zero mode of symmetric structures with $Al_{0.6}Ga_{0.4}As$ emitters (1) as well as for the zero (2), second (3), fourth (4), and sixth (5) modes of symmetric structures with $Al_{0.3}Ga_{0.7}As$ emitters.

decrease simultaneously the concentration of free charge carriers and the optical confinement factor of the active region. Nevertheless, when inequality

$$\Gamma_{\text{OW}}g_0 \gg \alpha_{\text{int}} + \alpha_{\text{ext}}$$
 (5)

is fulfilled, a small change in Γ_{QW} has little effect on the concentration of free charge carriers in the active region. In other words, when inequality (5) is valid, an increase in the waveguide thickness leading to a decrease in α_{QW} allows Γ_{QW} to be reduced. Therefore, the waveguide expansion is an efficient tool for decreasing the internal scattering losses from free carriers in the active region.

Figure 9 presents the total internal losses and internal optical losses in the active region of the symmetric SC DS versus the waveguide thickness [55]. The points show the experimental values of the total internal optical losses of the fundamental mode in 1.7- and 2.8-µm-thick asymmetric waveguide structures. One can see that the total internal losses for the given waveguide thicknesses in the asymmetric structure are almost equal to the losses of the fundamental mode in the symmetric structure. At waveguide thicknesses larger than 1 µm, the main fraction of the total losses is

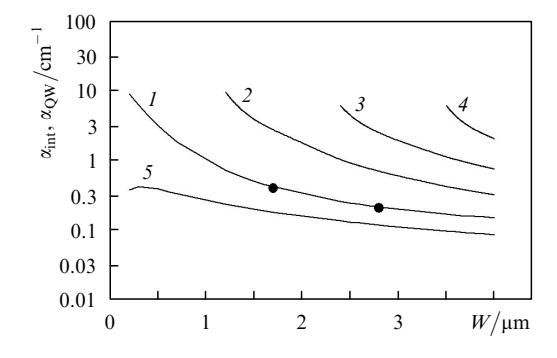


Figure 9. Dependences of the total internal optical losses α_{int} for the zero (1), second (2), fourth (4), and sixth (4) modes and of the internal optical active-region losses α_{QW} for the zero mode (5) on the waveguide thickness for symmetric heterostructures with $Al_{0.3}Ga_{0.7}As$ emitters. Points show the values of the total internal losses α_{int} of the zero mode of the heterostructures with an asymmetric position of the active region. The radiation wavelength is $\lambda=1.06~\mu m$.

accounted for by the internal optical losses $\alpha_{\rm QW}$ in the active region. They are completely determined by the threshold concentrations of charge carriers in the quantum well, whose lower limit is given by the transparency density of electrons n_0 and holes p_0 ; the values of the latter are determined by the properties of the active region material. Thus, the minimal internal optical losses calculated using the transparency densities $(0.2~{\rm cm}^{-1})$ are virtually the lower fundamental limit for 1- μ m heterostructure lasers with the active region (quantum well) consisting of InGaAs solid solutions [55].

2.4 High-power semiconductor lasers based on an asymmetric SC DH

The authors of papers [24, 62, 64–72] studied high-power semiconductor lasers with asymmetric separate-confinement heterostructures grown by the metal-organic vapour phase epitaxy method. The best results were achieved in a mesastripe laser Al-free heterostructure with a stripe width of 100 μ m. The laser structure contained the following epitaxial layers: heavily doped emitters N-Al_{0.3}Ga_{0.7}As ($N=10^{18}~{\rm cm}^{-3}$) and P-Al_{0.3}Ga_{0.7}As ($P=3.5\times10^{18}~{\rm cm}^{-3}$) and preliminary undoped 1.7- μ m-thick GaAs waveguide. The active region consisted of one InGaAs strained quantum well structure 90 Å in thickness; the electroluminescence wavelength was 1.08 μ m [64].

Figure 10 presents the inverse value of the external slope quantum efficiency as a function of the resonator length [64]. The internal quantum yield $\eta_{\rm int}$ of stimulated emission and internal optical losses $\alpha_{\rm int}$ in the lasers based on such heterostructures amounted to 99 % and 0.34 cm⁻¹, respectively [64]. The superlow internal optical losses obtained in this heterostructure make it possible to fabricate laser diodes with superlong resonators without a noticeable drop in the external slope quantum efficiency. An increase in the resonator length enables high currents to be used for laser diode pumping and, hence, the lasing power to be significantly increased while preserving the high conversion efficiency of electric energy into optical.

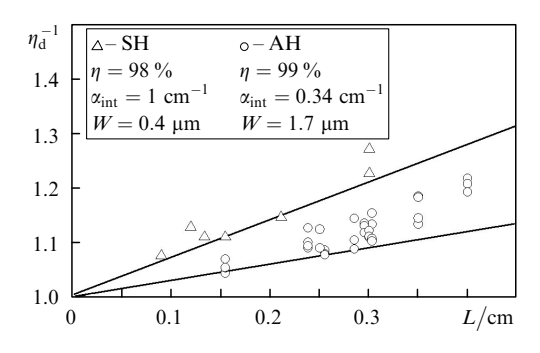


Figure 10. Experimental dependences of the inverse external slope quantum efficiency on the resonator length in a laser with a symmetric (SH) and asymmetric (AH) heterostructures.

The characteristic dependences of the lasing power and slope quantum efficiency on the pump current of a 3040- μ mlong laser diode resonator whose faces are HR- (95%) and AR-coated (5%) for the pump are presented in Fig. 11. The cw output power reached 16 W and the maximum value of η_d was 72% at the constant heat-sink temperature of 20°C [64].

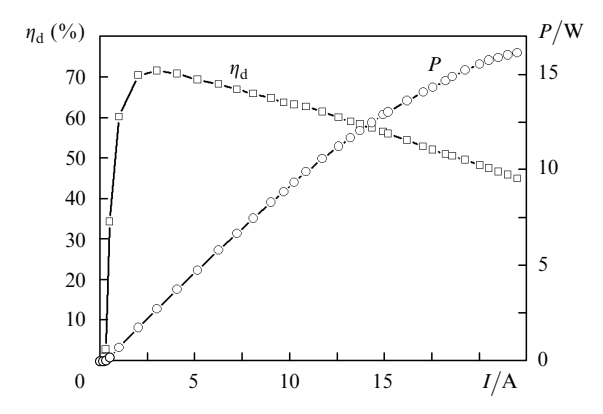


Figure 11. Light-current characteristic and dependence of the slope quantum efficiency on the pump current for a laser diode with the resonator length $L=3040~\mu m$ and the mesastripe width $D=100~\mu m$ with HR (95%) and AR (5%) coatings on the resonator end faces in the cw regime at a temperature of 20 °C.

The typical far-field radiation patterns in the plane perpendicular to the p-n junction at different values of the continuous pump current are shown in Fig. 12 [64]. Despite the expansion of the laser structure waveguide up to 1.7 μm , the angular width θ_{\perp} and shape of the radiation pattern virtually do not change with increasing the pump current. This stable behaviour of the radiation pattern indicates that the laser diode radiation is single mode in the plane perpendicular to the p-n junction, which is achieved due to the laser heterostructure asymmetry.

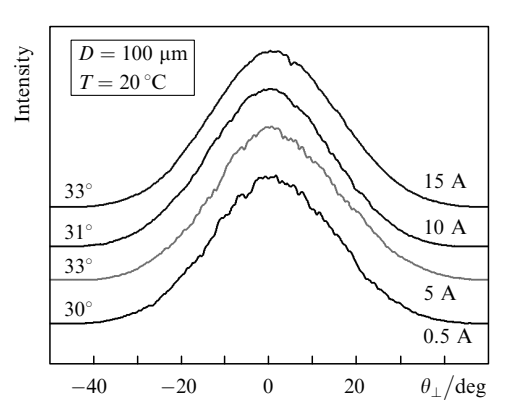


Figure 12. Dependences of the far-field intensity of cw radiation in the plane perpendicular to the p-n junction on the angle θ_{\perp} at different pump currents and angular widths of the half-intensity distribution of the field.

The emission spectra of a high-power semiconductor laser at different pump currents are shown in Fig. 13. The spectrum broadening can achieve 10 nm and in some cases even 15 nm. The reasons for this are as follows: an increase in the active region temperature [73], an increase in the threshold concentration of charge carriers outside the lasing threshold [74], and gain saturation due to the finiteness of the energy relaxation time of charge carriers [75].

Later the experiments aimed at increasing the output power were repeated and their results were improved in papers [76-80]. They all were obtained in laser heterostructures with small internal losses and very long resonators.

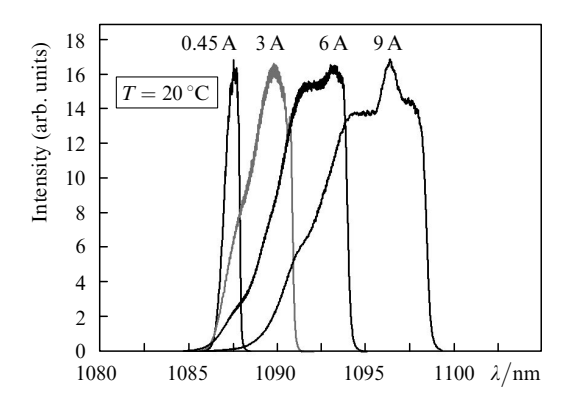


Figure 13. Emission spectra of a cw asymmetric heterostructure laser with a 1.7-µm-thick waveguide at different pump currents.

3. Temperature delocalisation of charge carriers in SC DHs

3.1 Overheating of the active region in a cw semiconductor laser

An increase in the output power of semiconductor lasers is one of the problems whose solution will allow one to extend the range of their application. This problem is the most challenging in the case of a cw laser. The light-current characteristic saturation limiting the output power in the cw regime results from the temperature rise in the active region. In cw high-power semiconductor lasers the temperature of laser heterostructure layers is higher than the heatsink temperature by tens of degrees. The active region overheating in the laser heterostructure can be recorded by measuring the shift of the long-wavelength tail of the emission spectrum envelope (Fig. 14) [73]. If the change in the position of the long-wavelength tail of the emission spectrum and its displacement temperature coefficient (3.3 Å deg^{-1}) [81] are known, we can determine the overheating of the active region with respect to the heat sink. The active region overheating depends not only on the pump current but also on the semiconductor laser efficiency and the thermal resistance ensured by the quality of metal coating deposition and its mounting on the heat-sink. For the standard efficiency of 55 % -65 % and the thermal resistance of $4-5 \text{ deg W}^{-1}$, the difference in the temper-

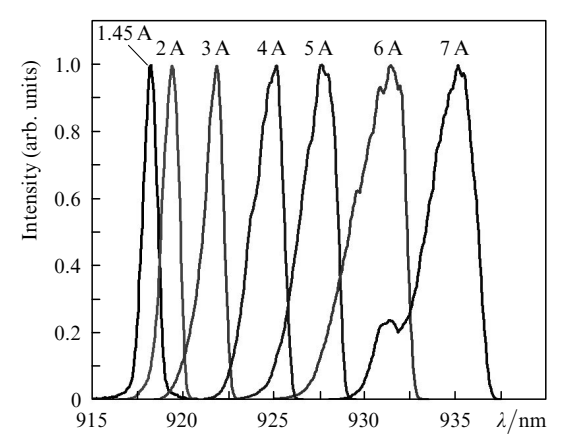


Figure 14. Emission spectra of a cw semiconductor laser at different pump currents.

atures between the active region and the heat sink is 30-50 °C, depending on the resonator length [73].

The active region overheating in the semiconductor laser can be reduced by increasing the efficiency, decreasing the thermal resistance, and increasing the stability temperature of the main laser parameters – the threshold current and external slope quantum efficiency.

3.2 Temperature dependence of internal optical losses

Expression (1) for the external slope quantum efficiency η_d includes the parameters leading to a decrease in η_d . These are the internal quantum yield of stimulated emission, internal optical losses, and external optical losses. For the given semiconductor laser, only the stimulated quantum yield and internal optical losses can change with increasing the pump current and the active region temperature. The experimental dependence of the inverse η_d on the resonator length L allows one to find the internal quantum yield of stimulated emission and total internal optical losses. Figure 15 presents the dependences $\eta_d^{-1}(L)$ for a semiconductor laser in the temperature range 20-140 °C in the pulsed pump regime (the pulse duration, $\tau = 0.5 - 1 \mu s$; pulse repetition rate, F = 1 kHz) [74]. The key feature of the dependences is the proximity to 100% for the internal quantum yield η_{int} of stimulated emission in the entire temperature range. It implies that when the pump current is increased and the active region of the laser heterostructure is overheated by 20-140 °C, no noticeable current leakage leading to a decrease in the external slope quantum efficiency emerges outside the lasing threshold. In turn, independence of η_{int} on temperature means that the lightcurrent characteristic in the cw regime is saturated due to an increase in the internal optical losses resulting from the active region overheating.

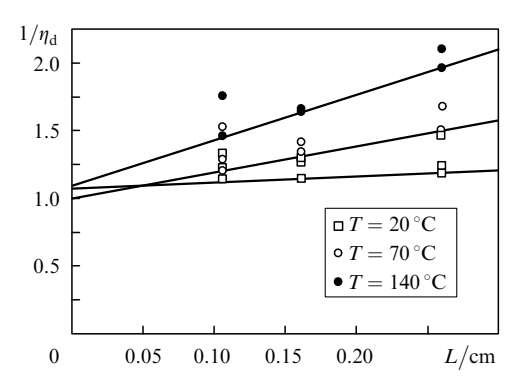


Figure 15. Dependences of the inverse slope quantum efficiency $1/\eta_{\rm d}$ on the resonator length L of pulsed heterostructure lasers at different temperatures.

The temperature dependence of the internal optical losses in the active region α_{QW} can be calculated taking into account the optical confinement factor Γ_{QW} by using expressions (2) and (3). Figure 16a shows the temperature dependences α_{QW} for three semiconductor laser heterostructures. In the first laser heterostructure based on a system of AlGaAs/InGaAs solid solutions, the active region is located between the intermediate GaAs layers. In the second laser heterostructure the active region is located directly between the AlGaAs waveguide layers. In the third laser heterostructure the number of quantum dots located between the

waveguide layers is increased up to four [74]. Figure 16b illustrates the temperature dependences of the total internal losses for the same laser heterostructures, these dependences being found from the dependence $\eta_d^{-1}(L)$ (Fig. 15) [74]. The total internal losses consisting of the losses in the active region layers, in waveguide layers and in P- and N-emitter layers [38, 55] exceed by several orders of magnitude the internal optical losses in the active region at the temperature of 140 °C. The use of asymmetric separate-confinement heterostructure with an expanded waveguide in high-power semiconductor lasers makes it possible to decrease the optical confinement factor in emitter layers down to less than 1.5 % [55, 64]; therefore, the temperature increase in the total internal losses should be determined by the increase in the losses in the active region and the waveguide layers of the laser heterostructure. To this end, the fraction of the internal optical losses in the waveguide layers dominates at high temperatures. Figure 17 presents the calculated temperature dependences of the charge carrier concentrations in the waveguide layers whose level can provide the observed internal optical losses and saturation of the light-current characteristic in high-power semiconductor lasers [74]. To saturate the light-current characteristic, it is sufficient to increase the charge carrier concentration from 3×10^{16} 3×10^{17} cm⁻³ in an expanded asymmetric waveguide.

The effect of temperature delocalisation and of an increase in the charge carrier concentration in the waveguide layers was discovered in lasers emitting at 1060–1100 nm [82]. One of the reasons for the temperature delocalisation is the small energy depth of quantum-well active regions in the

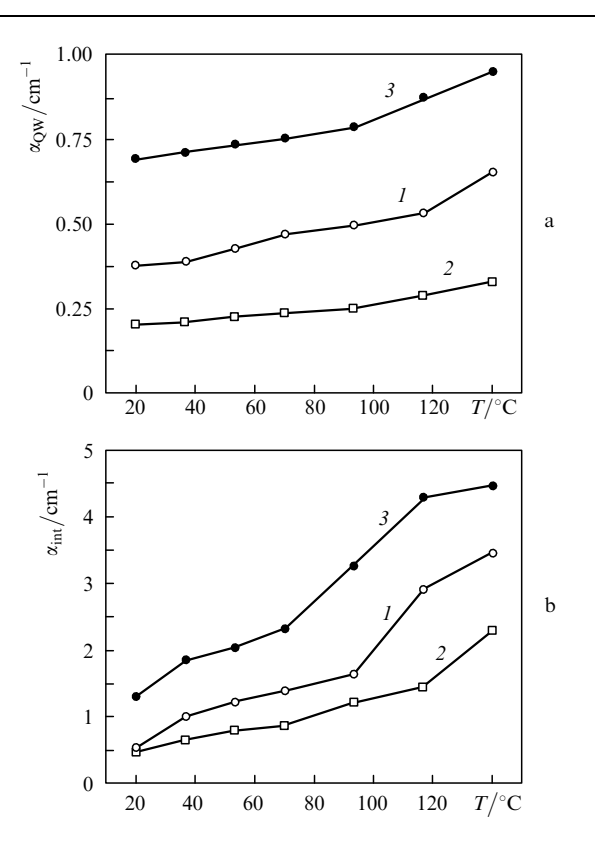


Figure 16. Temperature dependences of the internal optical losses in the active region (a) and the total optical losses (b) of semiconductor lasers made of heterostructures with an active region located between the intermediate GaAs layers (1), with an active region located between the AlGaAs waveguide layers (2) and with four quantum wells (3).

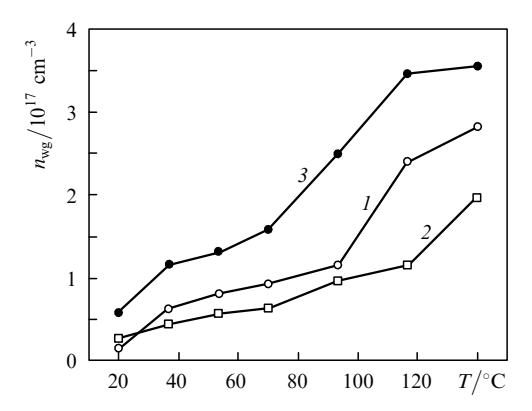


Figure 17. Temperature dependences of charge carrier concentrations n_{wg} in the waveguide layers of semiconductor lasers made of heterostructures with an active region located between the intermediate GaAs layers (1), with an active region located between the AlGaAs waveguide layers (2) and with four quantum wells (3).

laser heterostructure. The temperature rise leads to an increase in the threshold concentration of charge carriers and to their redistribution into high-energy states. As a result, the energy depth of active region quantum wells becomes insufficient to confine the charge carriers.

The effect of delocalisation and increase in the charge carrier concentration in the waveguide of lasers emitting at 900-920 nm is observed in studying the spontaneous emission spectra. Figure 18 shows the spontaneous recombination spectra for temperatures 20 and 140 °C [74]. At 140 °C the short wavelength wing of spontaneous emission spectrum is overlapped by the waveguide emission band. This means that the tails of the temperature distribution of electrons and holes are overlapped with the allowed states of the waveguide layer. As a result, not all the charge carriers required to achieve the threshold concentration are localised in the quantum well, and the waveguide layer is filled with delocalised charge carriers. At a temperature of 20 °C the short wavelength wing of spontaneous emission spectrum is not overlapped by the waveguide emission band, which means that delocalisation of charge carriers in the waveguide layers is absent. Because of temperature delocalisation of charge carriers in the waveguide layers of the laser heterostructures under study, the internal optical scattering losses from charge carriers increase in the waveguide layers [74, 83].

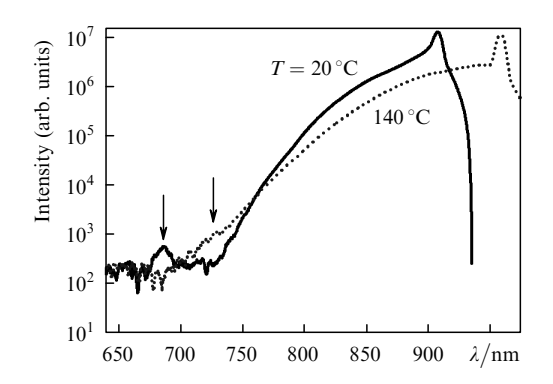


Figure 18. Spontaneous recombination spectra of a semiconductor laser at a pump current of 13 A and heat-sink temperatures of 20 and 140 °C. Arrorws show the emission bands of the waveguide.

4. Basic foundations of the concept of high-power semiconductor lasers

The displacement of the active region in the separate-confinement laser heterostructure allows one to suppress generation of higher-order modes due to a decrease in the optical confinement factors for these modes and to increase the waveguide thickness up to 4 μm and more. The waveguide expansion of the SC DH decreases the internal optical losses in the semiconductor laser at the lasing threshold almost down to the fundamental limit. In the cw regime, an increase in the pump current is accompanied by a rise of the laser heterostructure active region temperature with respect to the heat-sink temperature.

As a result, the threshold concentration of charge carriers increases and they are redistributed into high-energy states. The temperature spread of charge carriers with respect to the energy levels of the state density leads to charge carrier delocalisation in the waveguide layers of the laser SC DH, to an increase in the internal optical losses and as a result to a decrease in the slope quantum efficiency. The decrease in the latter results in light-current characteristic saturation of semiconductor lasers in the cw regime.

5. Internal quantum yield and effect of the active region thickness on this yield

Thus, the first basic foundation of the concept of highpower semiconductor lasers is the decrease in the internal optical losses and their preservation with increasing the pump current, especially in the cw regime.

The second basic foundation is the achievement of the maximal quantum yield of spontaneous luminescence in the active region of the laser heterostructure. Note that this requirement - common for all semiconductor lasers - is necessary and obligatory in designing high-power lasers. Unfortunately, its importance was underestimated because the internal quantum yield of stimulated emission can be close to 100 % at a significantly smaller internal quantum yield of spontaneous luminescence. The next misleading factor is the fact that in high-power semiconductor lasers the working pump current can exceed the threshold by 10-20times. Therefore, some (up to two twice) increase in the threshold current cannot substantially affect the working current quantity. However, this is valid only in the case if the threshold current density and the threshold concentration of charge carriers in the active region of the laser heterostructure do not increase. The internal optical losses and the probability of temperature delocalisation of charge carriers increase with increasing the threshold concentration, which leads to a decrease in the semiconductor laser output power.

The active region of an asymmetric SC DH most often represents a highly strained quantum-well epitaxial layer. The choice of the optimal thickness of the active region layer for each radiation wavelength is a challenging problem. To decrease the threshold current density it is needed to make the active region thicker in order to increase the optical confinement factor. The epitaxial layer thickness of the active region is limited by the critical layer thickness $H_{\rm cr}$ for the selected discrepancy of the lattice parameter, which can be calculated from the transcendental equation [82, 84]

$$H_{\rm cr} = \frac{b(1 - v\cos^2\varphi)}{2\pi f(1 + v)\sin\varphi\cos\theta} \left(\ln\frac{H_{\rm cr}}{b\sin\theta} + 1\right),\tag{6}$$

where v is the Poisson coefficient; b is the Burgers vector; ϕ is the angle between the Burgers vector and the line of discrepancy dislocation ($\phi = 60^{\circ}$); θ is the angle between the slip plane and the interphase boundary ($\theta = 54.74^{\circ}$); f is the discrepancy of the lattice periods between the layer and substrate.

Quite often the wavelength range of semiconductor lasers can be broadened by using compensating barriers, which control the relaxation of elastic stresses in the laser structure [85]. The use of barriers makes it possible to increase the thickness of the active region layer in an asymmetric laser SC DH with an expanded waveguide without increasing the internal optical losses of the laser. This is caused by the smallness of optical losses in the active region with respect to the total internal losses of the laser structure with superwide waveguide. Waveguide expansion in the separate-confinement laser structure above 1 µm leads to a decrease in the optical confinement factor in the active region down to the value of the order of the tenth fraction of percent. This circumstance allows one to vary the active region thickness in a wide range without violating the main requirement of the concept of high-power semiconductor lasers: not to increase the total internal losses. With increasing the active region thickness of the laser heterostructure (at a fixed composition of the solid solution, in particular, $In_xGa_{1-x}As$), we observe an improvement of such characteristics as the threshold current, temperature sensitivity of the threshold current density, stimulated quantum yield, and slope quantum efficiency [86]. The maximum possible optical output power increases with increasing the active region thickness up to values smaller than the critical one. At the active region thickness above $H_{\rm cr}$, the maximum possible optical output power drastically decreases, even to the point of lasing quenching. This is caused by the fact that the dependence of spontaneous internal quantum yield on the quantum-well epitaxial layer thickness of the active region has a maximum [86, 87] whose position depends on the solid-solution composition of the epitaxial layer of the active region. The greater the discrepancy between the lattice parameters of the active region layer and substrate, the more pronounced the maximum in the mentioned dependence (Fig. 19). Thus, the real critical

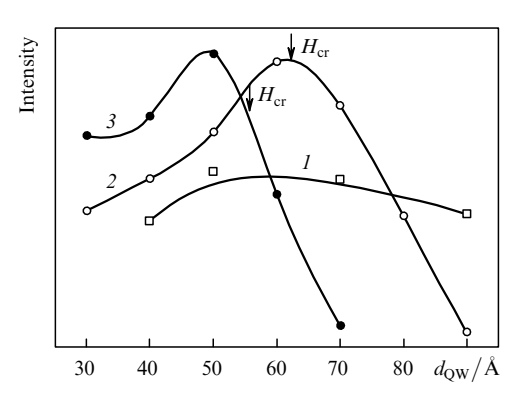


Figure 19. Dependences of the relative maximum intesnity of the photoluminescence spectrum on the $In_xGa_{1-x}As$ quantum-well layer thickness at x=0.28 (1), 0.39 (2), and 0.42 (3). Arrows show the critical active-region thickness $H_{\rm cr}$.

thickness of the active region is the thickness corresponding to the intensity maximum of photoluminescent emission [86, 87].

Therefore, waveguide expansion in an asymmetric laser SC DH allows one to decrease the internal optical losses and to optimise the active region thickness for obtaining the maximal quantum yield of spontaneous luminescence.

6. Catastrophic optical degradation and optical power density

An increase in the optical power of a semiconductor laser required some additional problems to be solved. At the output power of a cw laser above 5 W, catastrophic optical degradation of mirrors - damage of the Fabry-Perot resonator face due to the heating of the near-surface region of the active layer and substrate - begins. To some extent, the situation could be improved by depositing a dielectric coating on the resonator faces, which made it possible to increase the threshold of catastrophic optical degradation of mirrors. Most often the AR-coated output face of the Fabry – Perot resonator was degraded while the diode volt – ampere characteristic remained constant, and only in some cases (the development of catastrophic optical degradation of mirrors inside the epitaxial layers) there occurred an electrical breakdown of a semiconductor laser. The use of an expanded waveguide in the separate-confinement laser structure design and development of epitaxial technologies turned catastrophic optical degradation of mirrors into the main problem limiting an increase in the output power of a semiconductor laser.

This problem was studied in many papers [88–95]; however, because of commercial interests the results were often only stated at the initial stage of research and the physical problems leading to catastrophic optical degradation of mirrors were not yet touched upon. The authors of one of the first papers [88] studied in detail the local overheating of the active region caused by absorption of intrinsic radiation from a laser by the near-surface layer (depleted by nonequilibrium charge carriers) of the active region with an increased nonradiative recombination rate. The overheating of the near-surface region of the active layer of the structure with respect to the volume achieved several tens of degrees; in this case, it was maximal in laser structures containing aluminium in the waveguide and active region layers [88]. The AlGaAs solid solutions oxidise when in contact with the oxygen-containing atmosphere and get covered with an Al₂O₃ layer, the oxide layer being the larger the higher the aluminium content in the solid solution [96]. Under the oxide layer there are excess gallium and arsenic atoms which is an additional reason for radiation absorption and strengthening of nonradiative recombination processes, for the heating of the near-surface region, the decrease in the energy gap width, and the appearance of the positive feedback. An understanding of this process initiated studies of high-power Al-free semiconductor lasers [71, 73, 76, 97]. However, the technological development and increase in the output power of Al-containing semiconductor lasers negated the advantage of Al-free laser heterostructures due to which the cleaning and passivation technologies of resonator faces before depositing dielectric AR and HR coatings came to the fore.

One of the most efficient but highly expensive methods of deposition of such coatings is the so-called E2 process

[98]. Its distinctive feature is the cleaving in ultrahigh vacuum, accompanied by passivation or nitridization of cleaved faces of a resonator. The main advantage of this method consists in the fact that the oxide film is not removed from the surface of the cleaved face. High cost of the process and intricate equipment favoured the appearance of a number of cheap one-type approaches to the solution of the problem of surface cleaning from oxides and passivation of the Fabry-Perot resonator surface. The most wide-spread method [99] patented in Russia involves dry chemical etching by slow nitrogen ions in ultrahigh vacuum followed by passivation of the resonator face surface by nitrogen ions and a natural nitride layer. The method allows the cleavage of resonator faces in air, dry air, or dry nitrogen. The Al₂O₃ oxide is a sufficiently rugged oxide; therefore heavy and high-energy argon ions [100] as well as plasma [101] are used for the oxide removal. After it the surface is passivated to prevent its further oxidation. Most often use is made of nitridization accompanied by the formation of nitride in vitiated air; in this case, the smaller the oxygen content the more effective the nitridization process.

To protect the resonator faces in semiconductor lasers based on heterostructures free of aluminium in the semiconductor solid solution composition, another method can be employed, which does not require etching by high-energy ions. Indeed, etching by argon ions leads to a partial disturbance of the crystal structure of the resonator mirrors because the defects begin to form already at $\sim 10\text{-eV}$ ion energies. Oxides on the surfaces of Al-free semiconductor solid solutions have a smaller durability and chemical stability than aluminium oxides, which means that such surfaces can be cleaned by chemically active hydrogen ions [102]. Because the kinetic energy of the hydrogen ions being used does not exceed 1 eV, the surface of the resonator faces after its cleaning remains virtually free from defects.

Sometimes ZnSe is used instead of nitrides to passivate the cleaned faces. Rather good coincidence of the lattice parameters of this semiconductor with the parameters of GaAs and its compounds yields a beneficially low concentration of defects on the heterostructure boundary, at least on the segments of oxide-free mirror faces. ZnSe is deposited at low (below 300 °C) substrate temperatures from a Knudsen cell of a typical evaporator. The method allows the resonator cleaving in air, which makes it extremely low-cost and efficient; however, it cannot be employed to manufacture mirrors in lasers based on Al-containing solid solutions.

After the appearance of many patents devoted to surface cleaning and protection techniques, a number of papers were published which studied in detail the processes proceeding in the near-surface region of the active and waveguide layers. The authors of paper [103] presented the results of unique investigations of catastrophic optical degradation of mirrors in pulsed multimode semiconductor lasers. Using the resolution of ~ 7 µs they studied the nearfield dynamics and thermal distribution along the epitaxial layer of the active region. At the initial stage there was observed an absolute correlation between the measured characteristics: an increase in the intensity in the nearfield pattern corresponded to the temperature rise. A decrease in the power down to the spontaneous emission level indicated the place where catastrophic optical degradation of mirrors appeared. A no less detailed study of the

surface recombination and local overheating of the nearsurface region of the active region was performed in paper [104]. The authors of this paper demonstrated the correlation between the surface recombination intensity and the temperature rise in the near-surface region of the active laser heterostructure layer. These works again confirmed the validity and necessity of new cleaning and passivation technologies of laser resonator faces.

We should also mention investigations aimed at creation of a nonabsorbing window on the surface of a cleaved laser structure (see, for example, [105]). This direction in the studies has the right to exist and yields good results; however, it leads to complication and rise in the cost of a semiconductor laser: it is necessary to deposit a nonabsorbing layer on the cleaved region, to perform temperature mixing of the active layer in the near-surface region, to provide diffusion, etc. [106, 107].

One of the possible variants of the solution of the problem of catastrophic optical degradation of mirrors in high-power semiconductor lasers is the expansion of the laser heterostructure waveguide, which leads to a decrease not only in the internal optical losses but also in the power density at the resonator end face. An increase in the waveguide thickness by an order of magnitude, compared to the classical laser SC DH makes it possible to increase the output laser power also by an order of magnitude without changing the technology of dielectric coating deposition on resonator end faces. An experimental increase in the threshold of catastrophic optical degradation of mirrors up to 11 MW cm⁻² was achieved in lasers based on aluminiumcontaining semiconductor solid solutions [97], up to 40 MW cm⁻² – in lasers based on aluminium-free epitaxial layers [24]. A faster occurrence of catastrophic optical degradation of mirrors is observed sometimes in Al-free lasers most likely indicates some drawbacks in the technology used for coating deposition on the mirrors. The results of recent works using new mirror cleaning and passivation technologies in combination with an expanded waveguide decreasing the power density on the output resonator mirrors allowed the problem of catastrophic optical degradation of mirrors to be solved.

7. Quenching of lasing in semiconductor lasers with small internal optical losses

Development of the concept of high-power semiconductor lasers lead to the creation of laser SC DHs with superlow internal optical losses. The result was achieved due to waveguide expansion in the laser structure [25, 38, 55, 64, 68, 72], which resulted in a decrease both in the mode gain and in the internal optical losses in passive regions of the laser structure. A decrease in the mode gain was compensated for by an increase in the laser resonator length; however, the consequences of the decrease in the internal optical losses in passive regions were practically not studied. Interest in the internal optical losses in passive regions of pulsed and cw multimode semiconductor lasers appeared when standard means of combating quenching of lasing in high-power lasers of different stripe designs stopped working at high pump levels [108, 109]. Obviously, this effect was encountered by all researchers studying separate-confinement heterostructure lasers with small internal optical losses. However, in the context of the applied character of the problem the effect of quenching of lasing was not discussed in detail. An attempt to investigate this effect was done in paper [110]. The internal optical losses in the samples under study lied in the region between 0.4 and 0.6 cm⁻¹, the internal quantum yield of stimulated emission exceeded 90 %, i.e., with respect to the radiative efficiency the laser diodes were not inferior to the best known samples. Independently of the resonator length, most samples demonstrated a drastic, complete, or partial drop in the output power identified as quenching of lasing, this phenomenon being of reversible type and reproduced in repeated measurements. Figure 20 presents the typical light-current characteristics of semiconductor lasers with quenching of lasing [110]. In the radiation intensity distribution, the far field of the studied samples demonstrated a gradual increase in the radiation divergence from 5 to 14° with increasing the pump current. At the moment of quenching of lasing the far-field radiation pattern became consistent with the pattern in the near-threshold regime. Simultaneously, narrow peaks in the near-field intensity distribution of radiation in the direction perpendicular to the resonator axis were observed at the laser crystal end faces (Fig. 21). The maximum of the emission spectrum after quenching of lasing was shifted to the red, which indicates some decrease in the threshold current density and preservation of the lasing regime in mesastripe semiconductor lasers under study.

Based on the performed experiments, the authors of paper [110] made a conclusion that the threshold condition for the Fabry-Perot resonator modes is first fulfilled when the pump current is increased because the internal optical

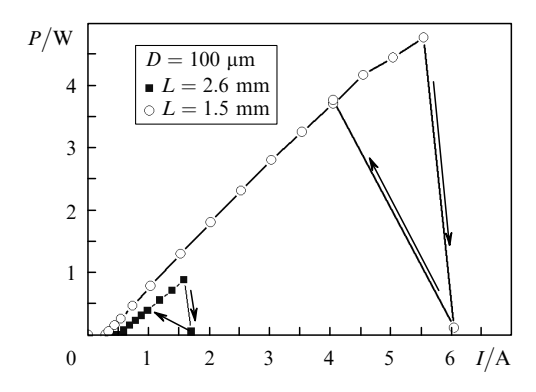


Figure 20. Dependence of the cw output power on the pump current for a semiconductor laser with AR- and HR-coated resonator end faces at resonator lengths of 1.5 and 2.6 mm.

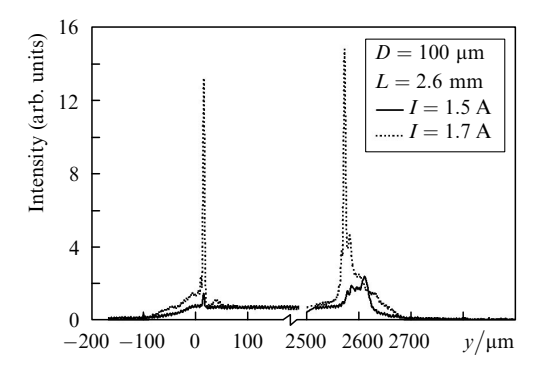


Figure 21. Intensity distribution of laser radiation on the crystal side face in the direction perpendicular to the radiation axis.

absorption losses are compensated for by radiation propagating directly in the waveguide. Passive regions unpumped by the current require additional bleaching by radiation scattered from a mesastripe waveguide. In laser heterostructures with a thin waveguide and internal losses achieving several tens of inverse centimetres an increase in the pump current does not lead to passive region bleaching. In laser heterostructures with a thick waveguide and internal optical losses less than one inverse centimetre the passive regions of a mesastripe laser heterostructure are bleached with increasing the pump current. The higherorder modes are characterised by the components propagating at a large angle to the stripe resonator axis. This increases manifold the fraction of scattered radiation propagating in passive regions of the laser. When some value of the pump current is achieved, the passive regions become bleached and the threshold lasing conditions are fulfilled for a closed ring mode of a four-sided resonator. Note that the lasing threshold of closed ring mode is always lower than that of any Fabry-Perot resonator mode, which results in quenching of lasing of the laser resonator modes.

The solution of the problem of laser quenching as well as the mounting of the laser crystal on a heat-sink refers to technological and design problems and is a 'know-how' of manufacturers of high-power semiconductor lasers who search for the most suitable processes of the laser fabrication. In solving this obvious (at first sight) problem aimed at prevention of closed ring mode emergence, one should take into account a rise in the cost and complication of the design, a decrease in the yield of active elements ready for operation from a wafer, an increase in the thermal resistance and total internal optical losses.

8. Pulsed semiconductor lasers

8.1 Pulsed lasing and fundamental limit of the optical power confinement of a semiconductor laser

For many years there has existed an unshakable axiom for all semiconductor lasers: when the lasing threshold is achieved, the charge carrier concentration stops increasing in the active region of the laser and the Fermi level is stabilised. This axiom was valid till the external conditions resulting from the development and creation of SC DH lasers changed: the working current density increased by 10–100 times, while the active laser region overheating with respect to the heat-sink reached 50-60 °C, which violated the charge carrier concentration stabilisation in the active region and the waveguide layer. First this phenomenon was discovered in paper [35] investigating the light-current and spectral parameters of SC DH semiconductor lasers. Summing up the results obtained in [35], it is pertinent to note that the average charge concentration in the waveguide layer of the laser structure continues to increase behind the lasing threshold with increasing the pump current; as a result, the light-current characteristic saturates. The authors of paper [111] studied the spectral characteristics of semiconductor lasers at pump current densities up to 60 kA cm⁻². The authors found that the spontaneous emission spectrum of the active region broadens and the charge carrier concentration increases behind the lasing threshold. Unfortunately, the samples of the semiconductor lasers were grown by the liquid epitaxy method, which presented problems in studying the emission

spectra. Later the authors of papers [112, 113] analysed in detail the effect of accumulation of current carriers in the pemitters, leading to an increase in the internal optical losses. The authors of paper [114] considered theoretically a temperature emission of current carriers into the waveguide from a quantum well, which explains the increase in the current leakage with increasing the pump level.

It took about ten years to improve the epitaxial technologies and understand the process proceeding in lasers, including the effect of temperature delocalisation of charge carriers into the waveguide layers due to active region overheating in the cw regime [73, 74], and to arm the researchers with laser samples grown by MOS hydride epitaxy [67]. This paper studied the properties of InGaAs/GaAS asymmetric heterostructure laser diodes under pulsed pumping ($\tau = 100 \text{ ns}, F = 1 - 10 \text{ kHz}$) by the current with the amplitude up to 200 A. The properties and characteristics of the used laser diodes under cw pumping were well studied [25, 38, 55, 64]. All the measurements in the pulsed regime were performed at room temperature. In the pulsed pump regime the maximal peak output power equal to 145 W was achieved (Fig. 22). Analysis of the emission spectra of the lasers in the case of different pulsed excitation levels showed that the spectrum width achieves 20-30 nm at high pump levels, the emission line being broadened not only to the red but also to the blue with increasing the current (Fig. 23). The temperature of the active region overheating is estimated to be 10-12 °C. The dependences of the near- and far-field intensity distributions of radiation in the laser diode showed

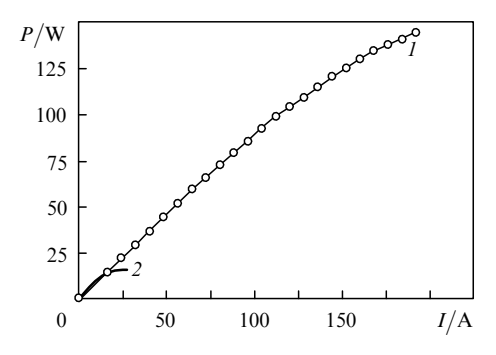


Figure 22. Light-current characterisite of a laser diode in the pulsed (1) and cw (2) pump regimes.

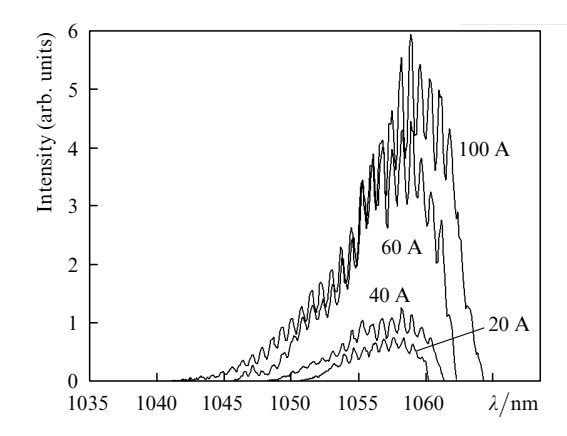


Figure 23. Emission spectra of a pulsed laser diode at different pump currents.

that lasing is uniformly distributed over the radiation region in the entire range of pump currents. The width of the far-field intensity distribution of radiation in the plane parallel to the p-n junction increases with increasing the pump current, which indicates the emergence of higher-order modes. The stable behaviour of the radiation pattern in the plane perpendicular to the p-n junction shows that the single-mode emission behaviour is retained.

The spectral and power parameters of near-IR semiconductor lasers ($\lambda = 1.01.8 \mu m$) at ultrahigh densities of pulsed pump currents were studied in detail in papers [75, 115, 116]. It was shown experimentally that the shift of the laser wavelength to the red is caused by an increase in the threshold current density and thus by an increase in the charge carrier concentration in the active region. It was found that in the pulsed pump regime the charge carrier concentration in the active region behind the lasing threshold increases by 6-7 times and can achieve 10^{19} cm⁻³ at current densities above 90 kA cm⁻² and laser densities above 100 MW cm⁻¹. The charge carrier concentration in the waveguide layers simultaneously increases with their concentration in the active region; in this case, the active region and the waveguide layers are sequentially filled with injected charge carriers. When the threshold concentration is achieved in the laser structure waveguide, an efficient channel of the recombination current leakage is activated and a drastic decrease in the slope quantum efficiency is observed.

The authors of paper [116] theoretically studied for the first time stimulated recombination processes when the charge carrier concentration increases behind the lasing threshold, and derived expressions for the stimulated recombination rate and time, the concentration of emitted photons, the quantum yield of stimulated emission, and the output laser power. The investigations performed prove that the light-current characteristic saturation of long-wavelength (1.3-1.8 µm) semiconductor lasers is explained by amplification of nonradiative recombination and by an increase in the optical losses caused by an increase in the carrier concentration in the active region of a heterostructure laser behind the lasing threshold at high excitation levels.

Thus, passage to the pulsed pump regime allows one to increase the output laser power almost by an order of magnitude while preserving all the main laser parameters. In the cw regime an increase in the active region temperature of a semiconductor laser by $50-60\,^{\circ}\mathrm{C}$ is the main reason of the light–current characteristic saturation. The maximum output power in the pulsed regime is the limit for the cw regime of a semiconductor laser with an ideal thermostabilisation system [67, 115, 117]. Nevertheless, at maximal pulsed pump levels we still observe the light–current characteristic saturation caused not only by the active region overheating.

8.2 Fundamental limit of the optical power confinement of a semiconductor laser

The effect of the light-current characteristic saturation in the pulsed regime was considered in detail in semiconductor lasers with a 100-µm-wide active region, the asymmetric separate-confinement heterostructures for these lasers being grown by MOS hydride epitaxy [75]. The properties and characteristics of these lasers were studied extensively in the cw regime [25, 55, 64]. Figure 24 presents the emission spectra of pulsed semiconductor lasers at different pump

currents. With increasing the pump current, we observe a shift of the long wavelength wing of the spectrum, caused by the active region heating during the current pulse, as well as the spectral broadening to the short wavelength region. At the pump current densities of $80-100 \text{ kA cm}^{-2}$, the emission spectral width achieved 60 nm in some cases. One more important feature in the spectrum behaviour is the saturation of its intensity maximum. After some level of the pump current is achieved, the laser intensity stops increasing and only the emission spectrum broadening is observed. The emission spectrum broadening up to 50-60 nm is possible only when the threshold conditions are fulfilled for the high-lying energy levels with respect to the levels participating already in lasing. To this end, the charge carrier concentration at high-lying levels should reach the threshold one.

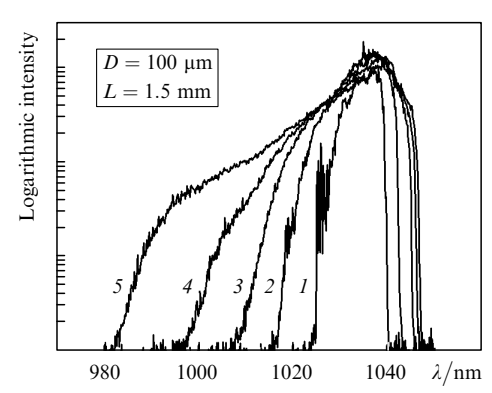


Figure 24. Emission spectra of a pulsed laser diode at pump current densities of 13 (1), 40 (2), 67 (3), 73 (4), and 80 kA cm⁻² (5).

The authors of papers [118, 119] considered the gain saturation effect in quantum-well heterostructures. The gain saturation in semiconductor lasers means the deviation from the linear law of the gain growth with current, typical of lasers with a volume active region. It was found empirically in quantum-well semiconductor lasers that the gain increases as a logarithm of threshold concentration [120]. However, the gain saturation with the increasing pump current cannot cause the saturation of the stimulated emission intensity because it is completely determined by the stimulated radiative recombination rate or the lifetime of charge carriers participating in stimulated radiative transitions. The stimulated radiative recombination rate is proportional to the number of injected carriers and the number of photons in the resonator; in this case, no physical reasons are obvious, which limit the growth of both parameters with increasing the pump current of the lasers. Therefore, according to the authors of [75] there should exist a fundamental reason leading to emission spectrum intensity saturation with increasing the pump current.

Following the quantum-mechanical approach to the energy scattering rate of charge carriers by polar optical phonons in a quantum well of a laser heterostructure [121, 122], the time of their scattering in the heterostructure under study can be approximately estimated as 2×10^{-11} s [75]. It is pertinent to note that the time of the electron energy scattering tends to increase with increasing the electron concentration [121].

Using the rate equations for electrons and photons [121] we can find the lifetime of stimulated radiative transitions:

$$\tau_{\text{stim}} = \frac{q N_{\text{QW}} V_{\text{QW}}}{\eta_{\text{int}} I},\tag{7}$$

where q is the electron charge; $N_{\rm QW}$ is the electron concentration in the active region; $V_{\rm QW}$ is the active region volume; I is the laser pump current. In the lasing regime the pump current is related to the laser power [120] by the expression

$$P = \eta_{\rm int} \frac{\alpha_{\rm ext}}{\alpha_{\rm int} + \alpha_{\rm ext}} \frac{hv}{q} (I - I_{\rm th}), \tag{8}$$

where hv is the photon energy; I_{th} is the threshold current of a semiconductor laser. By substituting η_{int}/q from (8) into (7) we can express the time of stimulated transition in a semiconductor laser by the laser output power, including that obtained experimentally. Figure 25 [curve (2)] illustrates the dependence of the lifetime of electrons participating in stimulated radiative recombination on the pump current density of a semiconductor laser [75]. In calculations the electron concentration was assumed equal to the threshold one $(5 \times 10^{18} \text{ cm}^{-3})$, and the internal quantum yield of stimulated emission was 100%. The behaviour of this dependence shows that in an ideal semiconductor laser, the lifetime of stimulated radiative recombination decreases with increasing the pump current. Figure 25 [curve (1)] demonstrates an analogous dependence calculated from experiemntal data [75]. The stimulated radiative recombination time begins stabilising after reaching $\sim 10^{-12}$ s.

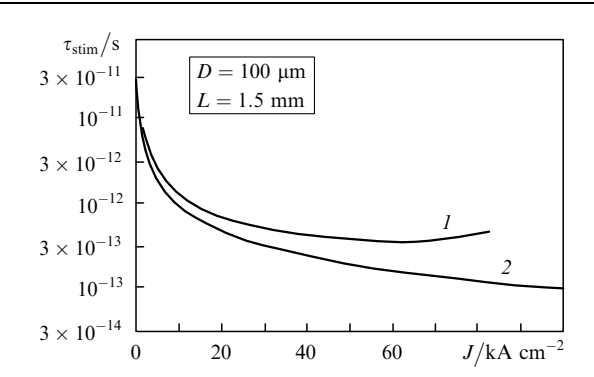


Figure 25. Dependences of the averaged stimulated lifetime of charge carriers in the quantum-well active region on the pump current density of the laser diode, calculated under the following assumptions: the threshold concentration of charge carriers in the active region increases with increasing the pump current (I) and the threshold concentration and the material gain are constant in the entire range of pump currents ($n_{\rm th} = 5 \times 10^{18} \ {\rm cm}^{-3}$, $G = 1600 \ {\rm cm}^{-1}$) (2).

Thus, the lifetime of charge carriers participating in the stimulated radiative recombination decreases and the radiation intensity increases with increasing the pump current behind the lasing threshold. At some pump current the lifetime of charge carriers participating in the stimulated radiative recombination becomes equal to the time of the electron energy scattering, and for some group of energy transitions the stimulated radiative recombination rate saturates. The concentration of charge carriers (electrons) at higher-lying levels increases and achieves the threshold value due to which the emission spectrum broadens. Then, with increasing the pump current the procedure is repeated

[75]. Note that the charge carrier concentration in the waveguide also increases due to an increase in the electron temperature in the active region [123].

The authors of paper [123] determined the concentration and temperature of hot electrons and holes as functions of the current density during spontaneous and stimulated emission in InGaAs/GaAs laser quantum-well separate confinement heterostructures. In the case of spontaneous emission, the concentration in the active region increases with increasing the current and the charge carrier temperature is small. In the case of stimulated emission, the situation is different. The concentration of injected carriers at rather small pump current densities (at currents exceeding the threshold one by several times) stabilises and does not increase with increasing the pump current, while the charge carrier temperature rises only by several degrees. At current densities exceeding the threshold density by factor of ten and hundred, there is no stabilisation: the concentration of charge carriers increases by several times and their temperature increases approximately up to 450 K at a 80-kA cm⁻² current density. The number of charge carriers injected from the active region to the barrier increases due to heating the charge carriers and due to an increase in their concentration in the active region. Theoretically this undesirable effect can be minimised by increasing the quantum-well depth [123]. However, this increase leads to an increase in the energy relaxation time of charge carriers especially when the concentration of hot electrons and holes increases.

8.3 Injection of charge carriers into the waveguide layer at high pump powers

The found increase in the charge carrier concentration in the active region leads to an increase in the current leakages. Figure 26 presents the dependence of the emission intensity from the waveguide layer of the laser heterostructure on the pump current, the dependence having two typical regions at current densities of 15 and 60 kA cm⁻². The first region refers to current densities at which the intensity maximum saturates in the emission spectrum. The second one refers to current densities corresponding to a drastic decrease in the slope quantum efficiency. When observing the emission behaviour along the resonator axis the second region coincides with the lasing threshold from the waveguide layers.

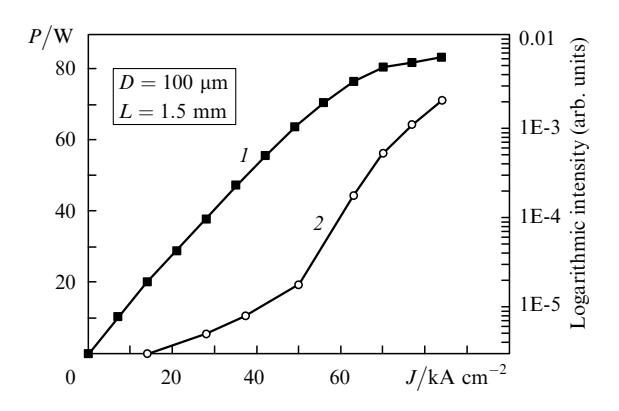


Figure 26. Dependences of the output power (1) and intensity of the luminescence spectrum maximum of the waveguide layer in the direction perpendicular to the resonator axis (2) on the pump current density of a pulsed laser diode at a temeprature of $20\,^{\circ}$ C.

The behaviour of the current leakages in the waveguide layer can be described by three processes corresponding to the regions with a sequentially increasing intensity. In the first region (with the smallest intensity), the radiative recombination in the waveguide adjacent to the p-emitter is proportional to current leakages from the active region and is determined by an excess concentration of the holes in this segment of the waveguide [35, 113]. In the second region, after the intensity maximum of the emission spectrum is saturated, the concentration in the active region begins to increase drastically and the injection of carriers to the waveguide layers also increases drastically [114]. As a result, the electron concentration increases in the waveguide adjacent to the p-emitter, and the current leakages in the form of the radiative recombination increase. In the third region, the electron injection in the waveguide layers increases with increasing the concentration in the active region. Experimentally this is confirmed by an increase in the emission intensity from the waveguide layers. This means that there opens an efficient channel of recombination current leakage from the active region. The lightcurrent characteristic demonstrates a break and a decrease in the slope quantum efficiency (Fig. 26).

An interesting effect related to an increase in the carrier concentration in the active region with increasing the pump level was found in [124]. Studying semiconductor lasers with a quantum-well active region containing two electronic quantum-dimensional levels it was elucidated that the integral emission spectrum consists of two bands (Fig. 27). The authors of [124] showed that the inverse population condition of the second electronic level and twoband lasing are achieved, first, due to a decrease in the stimulated lifetime at the first electronic level down to the quantity comparable with the relaxation time with respect to the electron energy in the active region, i.e., with the time of the electron delivery to the low-lying electronic level, and, second, due to a higher density of the states for the second electronic level than for the first level. Further investigations of the spectrum dynamics showed that when the conditions of the inverse population for the second electronic level are fulfilled, lasing from the first electronic level terminates [125].

We should also mention a series of works performed by very strong groups of researchers [80, 126, 127], who completely substantiated the results obtained by previous

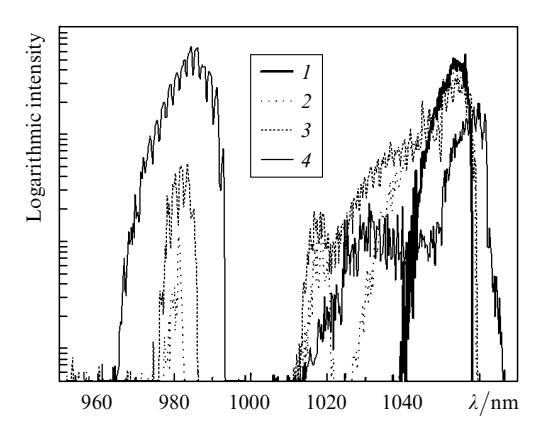


Figure 27. Integral emission spectrum of two-band laser diode with a 100-Å-thick quantum well, 1.5-mm-long resonator, 100- μ m-wide mesastripe in the pulsed regime at pump current densities of 13 (1), 35 (2), 80 (3), and 105 kA cm⁻² (4).

authors. Passage to the pulsed operation regime made it possible to increase the output power almost by an order of magnitude [80]. The main reason for the light-current characteristic saturation, i.e., an increase in the charge carrier concentration in the waveguide layers [80, 126], was confirmed. Unfortunately, the increase in the number of quantum wells in the laser SC DH with an effort to increase the total energy relaxation rate of charge carriers in quantum wells did not lead to an expected increase in the output power although the authors indicate the operation reliability improvement of such devices [126]. In paper [127] the authors analysed theoretically and experimentally the possible reasons for the light-current characteristic saturation in cw and pulsed semiconductor lasers.

8.4 Epitaxial tunnel-coupled laser structures

One of the methods for increasing the output power of pulsed semiconductor lasers is the fabrication of radiation sources based on epitaxial tunnel-coupled laser heterostructures [128–133]. Such a laser heterostructure design has a number of advantages. First, the output power can be increased manifold due to sequential integration of laser structures in one crystal. This technique is possible only for pulsed lasers because in the cw regime the active regions will be strongly overheated. The second advantage of tunnel-coupled laser heterostructures is a decrease in the pump current common for all the structures and an increase in the voltage on the laser crystal, which significantly simplifies fabrication of pulsed power sources with the current pulse duration of no less than 100 ns.

In designing epitaxial tunnel-coupled laser heterostructures two problems are solved: one technological process combines obtaining of a highly efficient tunnel p-n junction and production of an asymmetric separate confinement heterostructure with an expanded waveguide. A separate problem consists in the development of an active element of a stripe design consisting of two or three epitaxial tunnel-coupled laser structures.

An asymmetric SC DH with an expanded waveguide serves as a basis for high-power semiconductor lasers [38, 55, 66]. The internal optical losses in such a laser structure consist of a sum of losses in the active region, waveguide and emitter layers. Therefore, the doping level of emitter layers is chosen from the conditions of maintenance of efficient injection of positive and negative charge carriers and the minimal level of scattering losses by free charge carriers in the heavily doped emitter layers. A tunnel p-n junction is placed between the emitters of serially coupled structures in epitaxial tunnel-coupled laser structures. It was shown in paper [134] that a highly efficient p-n junction can be obtained by doping the GaAs layers by acceptors and donors up to the level $(8-9) \times 10^{19}$ cm⁻³. The use of acceptors (C) and donors (Si) as dopants makes it possible to obtain a sharp p-n junction caused by a small diffusion spread of profiles of both dopants.

It follows from general considerations that to optimise the after-growth operations related to the formation of a stripe structure of the active element, the thickness of the epitaxial tunnel-coupled laser structure should be minimised. The emitter thickness can be varied in epitaxial tunnel-coupled laser heterostructures because the waveguide thickness of an asymmetric separate-confinement structure is specified by the condition of minimal internal optical losses [38, 55, 66]. In paper [133] the emitter layer thick-

nesses were calculated based on the condition that the internal optical losses of this structure (due to propagation of radiation in the layers producing a tunnel p-n junction) do not exceed 5 %. The schematic energy band diagram of the structure and electromagnetic energy distribution in the waveguide of such a laser structure is presented in Fig. 28 [133]. Figure 29 shows the cleavage of the epitaxial tunnelcoupled laser heterostructure consisting of three asymmetric separate-confinement structures and grown by the MOS hydride epitaxy [133]. To ensure complete current confinement in all the sequential laser structures, the mesastripes limiting the waveguide of the active element were etched in a depth range of two or three laser structures. To remove uniformly and completely the etching products and to maintain the technological effectiveness of after-growth operations the mesastripes had a trapezoid form.

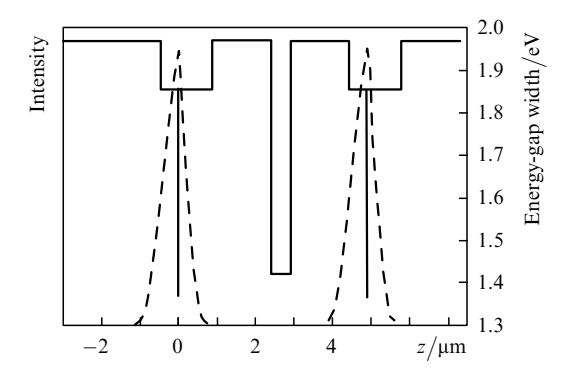


Figure 28. Schemetic of the energy band diagram of the epitaxial tunnel-coupled laser heterostructure (solid lines) and distribution of electromagentic radiation in the wavegudies of such a streuture (dashed curves).

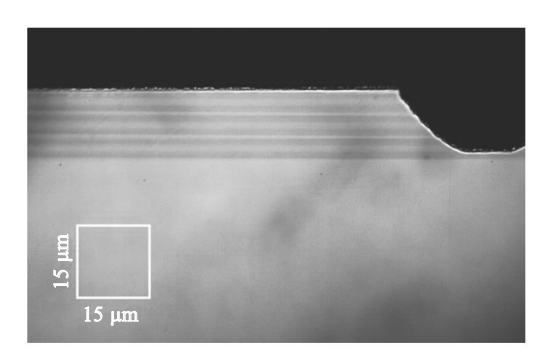


Figure 29. Photograph of a cleavage of a Fabry–Perot resonator of a mesastripe laser with three asymmetric separate-confinement heterostrucutres connected in series by tunnel p-n junctions.

Figure 30 presents the light-current characteristics for mesastripe lasers based on epitaxial tunnel-coupled laser structures [133]. Typical of the laser structures under study is an increase in the light-current characteristic slope by two (2 W A⁻¹) and three (3 W A⁻¹) times in comparison with single laser structures. In the samples the threshold current density amounted to $J_{\rm th}=96~{\rm A~cm}^{-2}$, the internal optical losses was estimated to be $\alpha_{\rm int}=0.82~{\rm cm}^{-1}$ and the slope resistance was $R=280~{\rm m\Omega}$ [133].

An especially interesting practical application of epitaxial tunnel-coupled structures is their use for designing two-stripe radiation sources [135, 136]. The authors of paper [137] showed the possibility of producing epitaxial tunnel-

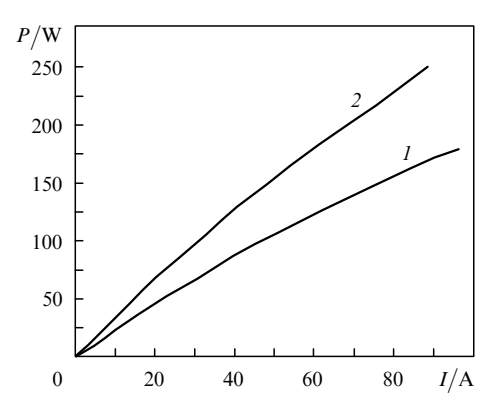


Figure 30. Light-current characteristics of mesastripe lasers based on epitaxial structures with one (1) and two (2) tunnel p-n junctions.

coupled laser heterostructures sequentially grown by MOS hydride epitaxy in one technological process and having different compositions of the active region solid solution. Mesastripe lasers with an aperture of 150×7 µm were fabricated from such structures and independent two-band lasing in one radiation source was obtained. The possibility of controlling the laser wavelength was demonstrated due to a change in the active region thickness in each tunnel-coupled laser structure. It was shown experimentally that in the pulsed regime the emission spectrum maxima in tunnel-coupled laser structures can shift up to 16 meV at an output power in each source up to 20 W [137].

9. High-power semiconductor lasers with a distributed Bragg mirror

One of the main applications of high-power semiconductor lasers is the pumping of solid-state optical systems. Such systems impose strict requirements to the parameters of pump lasers: output power, spectral range, and stability. Unfortunately, as was mentioned above the emission spectrum of a high-power semiconductor laser is shifted to the red and the worst of it is that its width increases with increasing the pump current. This drastically decreases the pump efficiency of solid-state elements. The desire to narrow down and stabilise the emission spectrum of a semiconductor laser made researchers return to the longknown design, i.e., distributed Bragg mirrors. The small depth of the electromagnetic-wave penetration into the emitter layers of the laser structure with an expanded waveguide as well as a considerable complication of the technology and a rise in the cost of a semiconductor laser were the main technological constraints.

The authors of papers [138, 139] were the first to show the possibility of obtaining the distributed feedback in a 975-nm multimode wide (100 µm) stripe laser. To provide a stable coefficient of the wave coupling, they made a heterostructure with a mode emitted into the emitter with a deposited diffraction grating. To do this, a layer with the refractive index close to the refractive index of the waveguide layer was placed inside the P-emitter. A 100-nm-thick second-order diffraction grating was produced by depositing a holographically exposed photoresist, followed by the displacement of this grating to a lower-lying level by the reactive ion etching. Then, the P-emitter layer and a contact layer were grown on the structure. As a result, a stunning result was achieved: single-mode lasing with a

 \sim 2.5-Å spectral width at an output power of 5 W and maximal efficiency of 53 % [138]. The temperature shift was in this case 0.065 nm K⁻¹. Unfortunately, the use of a holographic exposure followed by the layer deposition makes this method economically unreasonable.

Almost at the same time, the authors of [140] developed a more efficient variant of diffraction grating production in a laser structure of a single-mode mesastripe laser. In this variant the laser structure was not subjected to additional design changes. The six- or seven-order diffraction grating was deposited on a complete laser heterostructure coated by a photoresist with the help of standard photoligraphy at a wavelength of 365 nm. Then ~ 2 - μ m-deep reactive ion etching was performed. A distinctive feature of the active element of the semiconductor laser in this variant is the fact that the diffraction-grating region is isolated by a dielectric and is electrically passive. Practical realisation of this variant is obviously complicated because the same authors reported the creation of a multimode stripe laser with a distributed Bragg mirror only five years later [141]. To obtain the required reflection coefficient, the diffractiongrating length should achieve 500 µm, and the blaze-angle grating should be produced. This design allowed one to decrease the spectral width down to 1 nm in the entire range of output powers (up to 14 W) in the cw regime. The laser wavelength tuning was ~ 3.5 nm. In the quasi-cw regime the emission spectrum was broadened up to 1.5 nm, while the temperature frequency tuning was not observed up to the power of 23 W [141]. It is pertinent to note that the authors managed to preserve the internal optical losses at a 0.76cm⁻¹ level, which is a stunning achievement when introducing a 500-µm-long diffraction grating into the structure.

10. Conclusions. Fundamental, design, and technological factors affecting the limiting parameters of high-power semiconductor lasers

Thus, the concept of high-power semiconductor lasers consists of some requirements which should be fulfilled while designing such lasers. These requirements can be divided into three groups: technological, design, and fundamental.

To fulfill the technological requirements, one should have high-quality equipment and technologies of epitaxial deposition of nano-size and micron semiconductor layers, deposition of dielectric high-resistance coatings on Fabry—Perot resonator end faces, deposition of ohmic contacts on laser structures, and assembly of laser crystals on heat-sinks.

The level of perfection of molecular-beam MOS hydride technologies makes it possible to deposit epitaxial layers of a high crystallographic quality, which provides the leakage of high-density pump currents and heating up to high temperatures without defect formation.

The level of modern ultrahigh-vacuum equipment used to etch and deposit dielectric coatings allows one to achieve high optical resistance of dielectric mirrors deposited on the laser resonator end faces. The equipment should provide the possibility of preliminary removal of an oxide layer from the mirror surface and the possibility of the following passivation or provide the conditions for depositing dielectric coatings without mirror surface oxidation.

The level of modern technological equipment makes it possible to deposit homoheneous metal layers of a constant thickness and to provide the ohmic resistance of $20-50~\text{m}\Omega$.

If necessary the sequence of technological operations can ensure an additional increase in the level of semiconductor material doping due to sub-diffusion of the dopant.

The mentioned technological requirements are of no fundamental character because the both components of the technological process (technological equipment and manning level) can be perfected almost to infinity.

The design requirements of the concept of high-power semiconductor lasers consist of stringent conditions imposed on the separate-confinement laser heterostructure.

An asymmetric separate-confinement laser heterostructure with an expanded waveguide should provide a decrease in the internal optical losses down to the minimal possible level and conservation of lasing at the fundamental transverse mode of the expanded waveguide.

The thickness of the strained quantum-well active region should be selected from the condition ensuring the maximal quantum yield in the active region of the laser structure.

The energy depth of the active-region quantum well should be maximally increased in order to decrease the level of temperature delocalisation of the charge carriers from the active region.

The thickness and number of active-region quantum wells of an asymmetric separate-confinement laser heterostructure with an expanded waveguide should be maximally increased in order to increase the temperature stability of the threshold current density.

The basic requirements to the concept of high-power semiconductor lasers result from the fundamental reasons limiting the maximal output power. In the cw regime of laser operation the main reason is the heating of the laser crystal. In the pulsed regime of laser operation the fundamental reason limiting the output power is the finiteness of the energy relaxation of charge carriers in the active-region layer.

11. References

- Basov N.G., Krokhin O.N., Popov Yu.M. Zh. Eksp. Teor. Fiz., 40, 1879 (1961).
- Nasledov D.N., Rogachev A.A., Ryvkin S.M., Tsarenkov B.V. Fiz. Tverd. Tela, 4, 1062 (1962).
- Alferov Zh.I., Kazarinov R.F. Inventor's Certificate No. 181737 (1963).
- 4. Kroemer H. Proc. IEEE, 51, 1782 (1963).
- Alferov Zh.I., Andreev V.M., Garbuzov D.Z., Zhilyaev Yu.V., Morozov E.P., Trofim E.L. Fiz. Tekh. Poluprovodn., 4, 1826 (1970).
- Hayashi I., Panish M.B., Foy P.W., Sumski S. Appl. Phys. Lett., 17, 109 (1970).
- Van der Ziel J.P., Dingl R., Miller R.C., Wiegmann W., Nordlend W.A., Jr. Appl. Phys. Lett., 26, 463 (1975).
- 8. Tsang W.T. Appl. Phys. Lett., 40, 217 (1982).
- Dolginov L.M., Drakin A.E., Eliseev P.G., Sverdlov B.N., Skripkin B.A., Shevchenko E.G. Kvantovaya Electron., 11 (4), 645 (1984) [Sov. J. Quantum Electron., 7 (11), 439 (1984)].
- Alferov Zh.I., Garbuzov D.Z., Nivin A.B., Ovchinnikov A.V., Tarasov I.S. Pis'ma Zh. Tekh. Fiz., 19, 456 (1985).
- Alferov Zh.I., Garbuzov D.Z., Kizhaev K.Yu., Nivin A.B., Ovchinnikov A.V., Sokolova Z.N., Tarasov I.S. *Pis'ma Zh. Tekh. Fiz.*, 12, 210 (1986).
- Alferov Zh.I., Andereev V.M., Kazarinov R.F., Portnoi E.L., Suris R.A. Inventor's Certificate No. 392875 (1971).
- Alferov Zh.I., Gurevich S.A., Kazarinov R.F., Mizerov M.N., Portnoi E.L., Seisyan R.P., Suris R.A. Fiz. Tekh. Poluprovodn., 8, 832 (1974).
- Hirota O., Suematsu Y. IEEE J. Quantum Electron., QE-15, 142 (1979).

- Lang R., Kobayashi K. IEEE J. Quantum Electron., QE-16, 347 (1979).
- Kazarinov R.F., Suris R.A. Fiz. Tekh. Poluprovodn., 5, 707 (1971); 6, 120 (1972).
- Yonezu H., Sakuma I., Kobayashi K., Kamejima T., Ueno M., Nanishi Y. *Jpn. J. Appl.Phys.*, **12**, 1585 (1973).
- 18. Hakki B.W. J. Appl. Phys., 44, 5021 (1973).
- 19. Ho P.-T., Glasser L.A. Appl. Phys. Lett., 33, 241 (1978).
- 20. Ito H., Yokoyma H., Inaba H. Electron. Lett., 15, 738 (1979).
- Kurbatov L.N., Shakhidzhanov S.S., Bystrova L.V., Krapukhin V.V., Kolonenkova S.I. Fiz. Tekh. Poluprovodn., 4, 2025 (1970).
- Alphonse G.A., Gilbert D.B., Harvey M.G., Ettenberg M. IEEE J. Quantum Electron., 24, 2454 (1988).
- Alferov Zh.I., Antonichkis N.Yu., Arsent'ev I.N., Garbuzov D.Z., Kolyshkin V.I., Nalet T.A., Strugov N.A., Tikunov A.S. Fiz. Tekh. Poluprovodn., 22, 1031 (1988).
- Lifshits D.A., Egorov A.Yu., Kochnev I.V., Kapitonov V.A., Lantratov V.M., Ledentsov N.N., Nalet T.A., Tarasov I.S. Fiz. Tekh. Poluprovodn., 35 (3), 380 (2001).
- Pikhtin N.A., Slipchenko S.O., Sokolova Z.N., Stankevich A.L., Vinokurov D.A., Tarasov I.S., Alferov Zh.I. *Electron. Lett.*, 40 (22), 1413 (2004).
- 26. Tsang W.T. Appl. Phys. Lett., 40, 217 (1982).
- Alferov Zh.I., Vasil'ev A.I., Ivanov S.V., Kop'ev P.S., Ledentsov N.N., Lutsenko M.E., Mel'tser B.Ya., Ustinov V.M. Pis'ma Zh. Tekh. Fiz., 14, 1803 (1988).
- Alferov Zh.I., Andreev V.M., Aksenov V.Yu., Nalet T.A., Rumyantsev V.D., et al. *Pis'ma Zh. Tekh. Fiz.*, **14** (22), 2057 (1988).
- Alferov Zh.I., Arsent'ev I.N., Vavilova L.S., Garbuzov D.Z., Krasovskii V.V. Fiz. Tekh. Poluprovodn., 18 (9), 1655 (1984).
- Evtikhiev V.P., Garbuzov D.Z., Sokolova Z.N., Tarasov I.S., Khalfin V.B., Chalyi V.P., Chudinov A.V. Fiz. Tekh. Poluprovodn., 19 (8), 1420 (1985).
- 31. Alferov Zh.I., Garbuzov D.Z., Nivin A.B., Ovchinnikov A.V., Tarasov I.S. *Fiz. Tekh. Poluprovodn.*, **19** (3), 450 (1985).
- Alferov Zh.I., Garbuzov D.Z., Zaitsev S.V., Nivin A.B., Ovchinnikov A.V., Tarasov I.S. Fiz. Tekh. Poluprovodn., 21 (5), 824 (1987).
- Garbuzov D.Z., Chalyi V.P., Chudinov A.V., Svelokuzov A.E., Ovchinnikov A.V. Fiz. Tekh. Poluprovodn., 21 (3), 437 (1987).
- Garbuzov D.Z., Zaitsev S.V., Il'in Yu.V., Nalet T.A., Ovchinnikov A.V., Tarasov I.S. Pis'ma Zh. Tekh. Fiz., 16 (9), 50 (1990)
- Garbuzov D.Z., Ovchinnikov A.V., Pikhtin N.A., Sokolova Z.N., Tarasov I.S., Khalfin V.B. Fiz. Tekh. Poluprovodn., 25 (5), 928 (1991).
- Garbuzov D.Z., Antonichkis N.Y., Bondarev A.D.,
 Gulakov A.B., Zhigulin S.N., Katsavets N.I., Kochergin A.V.,
 Rafailov E.U. *IEEE J. Quantum Electron.*, 27, 1531 (1991).
- Al-Muhanna A., Mawst L.J., Botez D., Garbuzov D.Z., Martinelly R.U., Conolly J.C. Appl. Phys. Lett., 73, 1182 (1998).
- Pikhtin N.A., Slipchenko S.O., Sokolova Z.N., Tarasov I.S. Fiz. Tekh. Poluprovodn., 38, 374 (2004).
- Seeger K. Semiconductor Physics (Berlin: Springer, 1999; Moscow: Mir. 1977).
- 40. Fistul V.I. *Vvedenie v fiziku poluprovodnikov* (Introduction to Semiconductor Physics) (Moscow: Vyssh. Shkola, 1975).
- Casey H., Panish M. Heterostructure Lasers (New York: Acad. Press, 1978; Moscow: Mir, 1981) Vol. 1.
- Adachi S. Physical Properties of III–V Semiconductor Compounds (New Yjrk: John Wiley & Sons, 1992).
- 43. Nabiev R.F., Vail E.C., Chang-Hasnain C.J. *IEEE J. Quantum Electron.*, **31**, 234 (1995).
- Al-Muhanna A., Mawst L.J., Botez D., Garbuzov D.Z., Martinelly R.U., Conolly J.C. Appl. Phys. Lett., 62, 2402 (1993).
- He X., Srinivasan S., Wilson S., Mitchell C., Patel R. *Electron. Lett.*, 34, 2126 (1998).
- Livshits D.A., Kochnev I.V., Lantratov V.M., Ledentsov N.N., Nalet T.A., Tarasov I.S., Alferov Zh.I. Electron. Lett., 36, 1848 (2000).

- Bugge F., Erbert G., Fricke J., Gramlich S., Staske R., Wensel H., Zeimer U., Weyers M. Appl. Phys. Lett., 79, 1965 (2001).
- 48. Pikhtin N.A., Slipchenko S.O., Sokolova Z.N., Tarasov I.S. Fiz. Tekh. Poluprovodn., 36, 365 (2002).
- Kostko I.A., Evtikhiev V.P., Kotel'nikov E.Yu., Zegrya G.G. Fiz. Tekh. Poluprovodn., 33, 752 (1999).
- 50. kegami T. IEEE J. Quantum Electron., 8, 470 (1972).
- 51. Gordon E.I. IEEE J. Quantum Electron., 9, 772 (1973).
- 52. Krupka D.C. IEEE J. Quantum Electron., 11, 390 (1975).
- Levin L. IEEE Trans. Microwave Theory and Techniques, 23, 576 (1975).
- 54. Herzinger C.M., Lu C.C., DeTemple T.A., Chew W.C. *IEEE J. Quantum Electron.*, **29**, 2272 (1993).
- Slipchenko S.O., Vinokurov D.A., Pikhtin N.A., Sokolova Z.N., Stankevich A.L., Tarasov I.S., Alferov Zh.I. Fiz. Tekh. Poluprovodn., 38 (12), 1477 (2004).
- Shveikin V.I., Gelovani V.A. Kvantovaya Elektron., 32, 683 (2002)
 [Quantum Electron., 32, 683 (2002)].
- 57. Temmyo J., Sugo M. Electron. Lett., 31, 642 (1995).
- Vakhshoori D., Hobson W.S., Han H., Lopate J., Henein G.E., Wynn J.D., de Jong J., Schnoes M.L., Zydzik G.J. *Electron. Lett.*, 32, 1007 (1996).
- Verdiell J.M., Ziari M., Welch D.F. *Electron. Lett.*, 32, 1817 (1996).
- Zvonkov N.B., Akhlestina S.A., Ershov A.V., Zvonkov B.N., Maksimov G.A., Uskova E.A. Kvantovaya Elektron., 26, 217 (1999) [Quantum Electron., 29, 217 (1999)].
- Donnelly J.P., Huang R.K., Walpole J.N., Missaggia L.J., Harris C.T., Plant J.J., Bailey R.J., Mull D.E., Goodhue W.D., Turner G.W. IEEE J. Quantum Electron., 39, 289 (2003).
- Slipchenko S.O., Pikhtin N.A., Fetisova N.V., Khomylev M.A., Marmalyuk A.A., Nikitin D.B., Padalitsa A.A., Bulaev P.V., Zalevskii I.D., Tarasov I.S. *Pis'ma Zh. Tekh. Fiz.*, 29, 26 (2003).
- 63. Pinkas E., Miller B.I., Kayashi I., Foy P.W. IEEE J. Quantum Electron., 9, 281 (1973).
- Vinokurov D.A., Zorina S.A., Kapitonov V.A., Murashova A.V., Nikolaev D.N., Stankevich A.L., Khomylev M.A., Shamakhov V.V., Leshko A.Yu., Lyutetskiy A.V., Nalet T.A., Pikhtin N.A., Slipchenko S.O., Sokolova Z.N., Fetisova N.V., Tarasov I.S. Fiz. Tekh. Poluprovodn., 39 (3), 388 (2005).
- Andreev A.Yu., Leshko A.Yu., Lyutetskiy A.V., Marmalyuk A.A., Nalet T.A., Padalitsa A.A., Pikhtin N.A., Sabitov D.R., Simakov V.A., Slipchenko S.O., Khomylev M.A., Tarasov I.S. Fiz. Tekh. Poluprovodn., 40 (5), 628 (2006).
- Vinokurov D.A., Stankevich A.L., Shamakhov V.V., Kapitonov V.A., Leshko A.Yu., Lyutetskiy A.V., Nikolaev D.N., Pikhtin N.A., Rudova N.A., Sokolova Z.N., Slipchenko S.O., Khomylev M.A., Tarasov I.S. Fiz. Tekh. Poluprovodn., 40 (6), 764 (2006)
- Vinokurov D.A., Kapitonov V.A., Lyutetskiy A.V., Nikolaev D.N., Pikhtin N.A., Rozhkov A.V., Rudova N.A., Slipchenko S.O., Stankevich A.L., Fetisova N.V., Khomylev M.A., Shamakhov V.V., Borshchev K.S., Tarasov I.S. Pis'ma Zh. Tekh. Fiz., 32 (16), 47 (2006).
- Lyutetskiy A.V., Borshchev K.S., Bondarev A.D., Nalet T.A., Pikhtin N.A., Slipchenko S.O., Fetisova N.V., Khomylev M.A., Marmalyuk A.A., Ryaboshtan Yu.L., Simakov V.A., Tarasov I.S. Fiz. Tekh. Poluprovodn., 41 (7), 883 (2007).
- Andreev A.Yu., Zorina S.A., Leshko A.Yu., Lyutetskiy A.V., Marmalyuk A.A., Murashova A.V., Nalet T.A., Padalitsa A.A., Pikhtin N.A., Sabitov D.R., Simakov V.A., Slipchenko S.O., Telegin K.Yu., Shamakhov V.V., Tarasov I.S. Fiz. Tekh. Poluprovodn., 43 (4), 543 (2009).
- Kim Y.S., Kang D.H., Lee C.Y. Fiz. Tekh. Poluprovodn., 42 (7), 882 (2008).
- Bezotosnyi V.V., Vasil'eva V.V., Vinokurov D.A., Kapitonov V.A., Krokhin O.N., Leshko A.Yu., Lyutetskiy A.V., Murashova A.V., Nalet T.A., Nikolaev D.N., Pikhtin N.A., Popov Yu.M., Slipchenko S.O., Stankevich A.L., Fetisova N.V., Shamakhov V.V., Tarasov I.S. Fiz. Tekh. Poluprovodn., 42 (3), 357 (2008).

- Aluev A.V., Leshko A.Yu., Lyutetskiy A.V., Pikhtin N.A., Slipchenko S.O., Fetisova N.V., Chel'nyi A.A., Shamakhov V.V., Simakov V.A., Tarasov I.S. Fiz. Tekh. Poluprovodn., 43 (4), 556 (2009).
- Ladugin M.A., Marmalyuk A.A., Padalitsa A.A., Pikhtin N.A., Podoskin A.A., Rudova N.A., Slipchenko S.O., Shashkin I.S., Bondarev A.D., Tarasov I.S. Fiz. Tekh. Poluprovodn., 44 (10), 1417 (2010).
- Pikhtin N.A., Slipchenko S.O., Shashkin I.S., Ladugin M.A., Marmalyuk A.A., Podoskin A.A., Tarasov I.S. Fiz. Tekh. Poluprovodn., 44 (10), 1411 (2010).
- Slipchenko S.O., Sokolova Z.N., Pikhtin N.A., Borshchev K.S., Vinokurov D.A., Tarasov I.S. Fiz. Tekh. Poluprovodn., 40 (8), 1017 (2006).
- Kanskar M., Earles T., Goodnough T.J., Stiers E., Botez D., Mawst L.J. *Electron. Lett.*, 41 (5), 245 (2005).
- Knigge A., Erbert G., Jonsson J., Pittroff W., Staske R., Sumpf B., Weyers M., Trankle G. Electron. Lett., 41 (5), 250 (2005).
- Pietrzak A., Wenzel H., Erbert G., Tränkle G. Opt. Lett., 33 (19), 2188 (2008).
- Crump P., Blume G., Paschke K., Staske R., Pietrzak A., Zeimer U., Einfeldt S., Ginolas A., Bugge F, Häusler K., Ressel P., Wenzel H., Erbert G. Proc. SPIE Int. Soc. Opt. Eng., 7198, 719814 (2009).
- Pietrzak A., Crump P., Wenzel H., Staske R., Erbert, G., Tränkle G. Semicond. Sci. Technol., 24, 035020 (2009).
- Diehl R. High-Power Diode Lasers: Fundamentals, Technology, Applications (Berlin: Springer, 2000).
- 82. Matthews J.W. The J. Vacuum Sci. Technol., 12, 126 (1975).
- Slipchenko S.O., Shashkin I.S., Vavilova L.S., Vinokurov D.A., Lyutetskiy A.V., Pikhtin N.A., Podoskin A.A., Stankevich A.L., Fetisova N.V. Tarasov I.S. Fiz. Tekh. Poluprovodn., 44 (5), 688 (2010)
- Matthews J.W., Mader S., Light T.B. J. Appl. Phys., 41, 3800 (1970).
- Shamakhov V.V., Vinokurov D.A., Stankevich A.L., Kapitonov V.A., Zorina S.A., Nikolaev D.N., Murashova A.V., Tarasov I.S. *Pis'ma Zh. Tekh. Fiz.*, 31 (23), 1 (2005).
- Vinokurov D.A., Vasil'eva V.V., Kapitonov V.A., Lyutetskiy A.V., Nikolaev D.N., Pikhtin N.A., Slipchenko S.O., Stankevich A.L., Shamakhov V.V., Fetisova N.V., Tarasov I.S. Fiz. Tekh. Poluprovodn., 44, 246 (2010).
- Vinokurov D.A., Kapitonov V.A., Nikolaev D.N., Sokolova Z.N., Stankevich A.L., Shamakhov V.V., Tarasov I.S. Fiz. Tekh. Poluprovodn., 43, 1374 (2009).
- Alferov Zh.I., Katsavets N.I., Petrikov V.D., Tarasov I.S., Khalfin V.B. Fiz. Tekh. Poluprovodn., 30 (3), 474 (1996).
- Henry C.H., Petroff P.M., Logan R.A., Merrit F.R. J. Appl. Phys., 50, 3721 (1979).
- 90. Todoroki S., Sawai M., Aiki K. J. Appl. Phys., 58, 1124 (1985).
- 91. Brugger H., Epperlein P.W. Appl. Phys. Lett., 56, 1149 (1990).
- Tang W.C., Rosen H.J., Vettiger P., Webb D.J. Appl. Phys. Lett., 58, 557 (1991).
- Yoo J.S., Lee H.H., Zory P. IEEE J. Quantum Electron., 28, 635 (1992).
- 94. Cole J.V., Lee H.H. IEEE J. Quantum Electron., 29, 322 (1993).
- 95. Chen G., Tien C.L. J. Appl. Phys., 74, 2167 (1993).
- Ankudinov A.V., Evtikhiev V.P., Tokranov V.E., Ulin V.P., Titkov A.N. Fiz. Tekh. Poluprovodn., 33 (5), 594 (1999).
- 97. Botez D. Compound Semiconductors, 5 (6), 24 (1998).
- Gasser M., Latta E.E. Method for Mirror Passivation of Semiconductor Laser Diodes, US Patent 5 144 634, Sep. 1, 1992.
- Lindstrom L.K., Blikst P.N., Sederholm S., Srinivasan A., Karlstrom K.-F. Patent No. 2303317 dated 09.08.2002.
- Kawazu Z., Tashiro Y., Shima A., Suzuki D., Nishiguchi H., Yagi T., Omura E. *IEEE J. Selected Topics in Quantum Electron.*, 7 (2), 184 (2001).
- Hirotaka O., Hideyoshi H., Toshinari F. Compound Semiconductor Light Emitting Device, European Patent EP1 006 629, Jul. 7, 2000.

 Ressel P., Erbert G., Zeimer U., Häusler K., Beister G., Sumpf B., Klehr A., Tränkle G. *IEEE Photon. Technol. Lett.*, 17 (5), 962 (2005).

- Ziegler M., Tomm J.W., Reeber D., Elsaeeser T., Zeimer U., Larsen H.E., Petersen P.M., Andersen P.E. Appl. Phys. Lett., 94, 191101 (2009).
- Ziegler M., Talalaev V., Tomm J.W., Elsaeeser T., Ressel P.,
 Sumpf B., Erbert G. Appl. Phys. Lett., 92, 203506 (2008).
- Lammert R.M., Osowski M.L., Oh S.W., Panja C., Ungar J.E. Electron. Lett., 42 (9) 535 (2006).
- Walker C.L., Bryce A.C., Marsh J.H. *IEEE Photonics. Technol. Lett.*, 14 (10), 1394 (2002).
- 107. Marsh J. Semicond. Sci. Technol., 8, 1136 (1993).
- Komissarov A., Maiorov M., Menna R., Todorov S., Connolly J., Garbuzov D., Khalfin V., in *Proc. Conf. CLEO'2001* (Baltimore, 2001) Paper CMG1.
- Leshko A.Yu., Lyutetskiy A.V., Pikhtin N.A., Slipchenko S.O., Sokolova Z.N., Fetisova N.V., Golikova E.G., Ryaboshtan Yu.A., Tarasov I.S. Fiz. Tekh. Poluprovodn., 36, 1393 (2002).
- Slipchenko S.O., Vinokurov D.A., Lyutetskiy A.V., Pikhtin N.A., Stankevich A.L., Fetisova N.V., Bondarev A.D., Tarasov I.S. Fiz. Tekh. Poluprovodn., 43 (10), 1409 (2009).
- Pikhtin N.A., Tarasov I.S., Ivanov M.A. Fiz. Tekh. Poluprovodn., 28 (11), 1983 (1994).
- 112. Ryvkin B.S., Avrutin E.A. J. Appl. Phys., 97, 123103 (2005).
- 113. Ryvkin B.S., Avrutin E.A. J. Appl. Phys., 97, 113106 (2005).
- Asryan L.V., Gun'ko N.A., Polkovnikov A.S., Zegrya G.G., Suris R.A., Lau P-K., Makino T. Semicond. Sci. Technol., 15, 1131 (2000).
- 115. Vinokurov D.A., Kapitonov V.A., Lyutetskiy A.V., Pikhtin N.A., Slipchenko S.O., Sokolova Z.N., Stankevich A.L., Khomylev M.A., Shamakhov V.V., Borshchev K.S., Arsent'ev I.N., Tarasov I.S. Fiz. Tekh. Poluprovodn., 41 (8), 1003 (2007)
- Lyutetskiy A.V., Borshchev K.S., Pikhtin N.A., Slipchenko S.O., Sokolova Z.N., Tarasov I.S. Fiz. Tekh. Poluprovodn., 42 (1), 106 (2008).
- 117. Tarasov I.S., Pikhtin N.A., Slipchenko S.O., Sokolova Z.N., Vinokurov D.A., Kapitonov V.A., Khomylev M.A., Leshko A.Yu., Lyutetskiy A.V., Stankevich A.L. Spectrochim. Acta, Pt A, 66, 819 (2007).
- Zegrya G.G., Solov'ev I.Yu. Fiz. Tekh. Poluprovodn., 39, 636 (2005).
- Garbuzov D.Z., Tikunov A.V., Khalfin V.B. *Fiz. Tekh. Poluprovodn.*, 21, 1085 (1987).
- Coldren L.A., Corzine S.W. Diode Lasers and Photonic Integrated Circuits (New York: John Wiley and Sons, 1995).
- 121. Vorob'ev L.E., Danilov S.N., Zerova V.L., Firsov D.A. Fiz. Tekh. Poluprovodn., 37, 604 (2003).
- 122. Vorob'ev L.E., Danilov S.N., Ivchenko E.L., Levinshtein M.E., Firsov D.A., Shalygin V.A. Kineticheskie i opticheskie yavleniya v sil'nykh elektricheskikh polyakh v poluprovodnikovykh nanostrukturakh (Kinetic and Optical Phenomena in Strong Electric Fields in Semiconductor Nanostructures) (St. Petersburg: Nauka, 2000).
- Vorob'ev L.E., Zerova V.L., Borshchev K.S., Sokolova Z.N., Tarasov I.S., Belenky G. Fiz. Tekh. Poluprovodn., 42, 753 (2008).
- 124. Vinokurov D.A., Zorina S.A., Kapitonov V.A., Leshko A.Yu., Lyutetskiy A.V., Nalet T.A., Nikolaev D.N., Pikhtin N.A., Slipchenko S.O., Sokolova Z.N., Stankevich A.L., Rudova N.A., Fetisova N.V., Khomylev M.A., Shamakhov V.V., Borshchev K.S., Arsent'ev I.N., Bondarev A.D., Trukan M.K., Tarasov I.S. Fiz. Tekh. Poluprovodn., 41, 1247 (2007).
- 125. Sokolovskii G.S., Vinokurov D.A., Deryagin A.G., Dyudelev V.V., Kuchinskii V.I., Losev S.N., Lyutetskiy A.V., Pikhtin N.A., Slipchenko S.O., Sokolova Z.N., Tarasov I.S. Pis'ma Zh. Tekh. Fiz., 34 (16), 58 (2008).
- 126. Wang X., Crump P., Pietrzak A., Schultz C., Klehr A., Hoffmann T., Liero A., Ginolas A., Einfeldt S., Bugge F., Erbert G., Tränkle G. Proc. SPIE Int. Soc. Opt. Eng., 7198, 71981G-1 (2009).

- Wenzel H., Crump P., Pietrzak A., Roder C., Wang X., Erbert G. Optical and Quantum Electron., DOI 10.1007/s11082-010-9372-4 (2010).
- Van der Ziel J.P., Tsang W.T. Appl. Phys. Lett., 41 (6), 499 (1982).
- Garcia J.Ch., Rosencher E., Collot Ph., Laurent N., Guyaux J.L.,
 Vinter B., Nagle J. Appl. Phys. Lett., 71 (26), 3752 (1997).
- Patterson S.G., Petrich G.S., Ram R.J., Kolodziejski L.A. Electron. Lett., 35, 395 (1999).
- Hanke C., Korte L., Acklin B.D., Behringer M., Herrmann G., Luft J., et al. Proc. SPIE Int. Soc. Opt. Eng., 3947, 50 (2000).
- Vinokurov D.A., Ladugin M.A., Marmalyuk A.A., Padalitsa A.A., Pikhtin N.A., Simakov V.A., Sukharev A.V., Fetisova N.V., Shamakhov V.V., Tarasov I.S. Fiz. Tekh. Poluprovodn., 43 (9), 1253 (2009).
- Zverkov M.V., Konyaev V.P., Krichevskii V.V., Ladugin M.A.,
 Marmalyuk A.A., et al. *Kvantovaya Elektron.*, 38 (11), 989 (2008)
 [Quantum Electron., 38 (11), 989 (2008)].
- Vinokurov D.A., Konyaev V.P., Ladugin M.A., Lyutetskiy A.V., Marmalyuk A.A., Padalitsa A.A., Petrunov A.N., Pikhtin N.A., Simakov V.A., Slipchenko S.O., Sukharev A.V., Fetisova N.V., Shamakhov V.V., Tarasov I.S. Fiz. Tekh. Poluprovodn., 44 (2), 251 (2010).
- Hoffmann S., Hofmann M., Kira M., Koch S.W. Semicond. Sci. Technol., 20, S205 (2005).
- Wilk R., Klehr A., Mikulics M., Hasek T., Walther M., Koch M. Electron. Lett., 43, 108 (2007).
- Vinokurov D.A., Ladugin M.A., Lyutetskiy A.V., Marmalyuk A.A., Petrunov A.N., Pikhtin N.A., Slipchenko S.O., Sokolova Z.N., Stankevich A.L., Fetisova N.V., Shashkin A.S., Averkiev N.S., Tarasov I.S. Fiz. Tekh. Poluprovodn., 44 (6), 833 (2010).
- Kanskar M., He Y., Cai J., Galstad C., Macomber S.H.,
 Stiers E., Botez D., Mawst L.J. *Electron. Lett.*, **42** (25), 14455 (2006)
- Chang C.H., Earles T., Botez D. Electron. Lett., 36 (11), 954 (2000).
- Fricke J., Wenzel H., Matalla M., Klehr A., Erbert G. Semicond. Sci. Technol., 20, 1149 (2005).
- Fricke J., Bugge F., Ginolas A., John W., et al. *IEEE Photon. Tehnol. Lett.*, 22 (5), 284 (2010).